SAND2014-17909PE

NMR Relaxation Studies at Sandia National Labs

Roger Assink
Sandia National Labs
(retired)

Molecular Dynamics of Octane in a Gas Liquid Solution

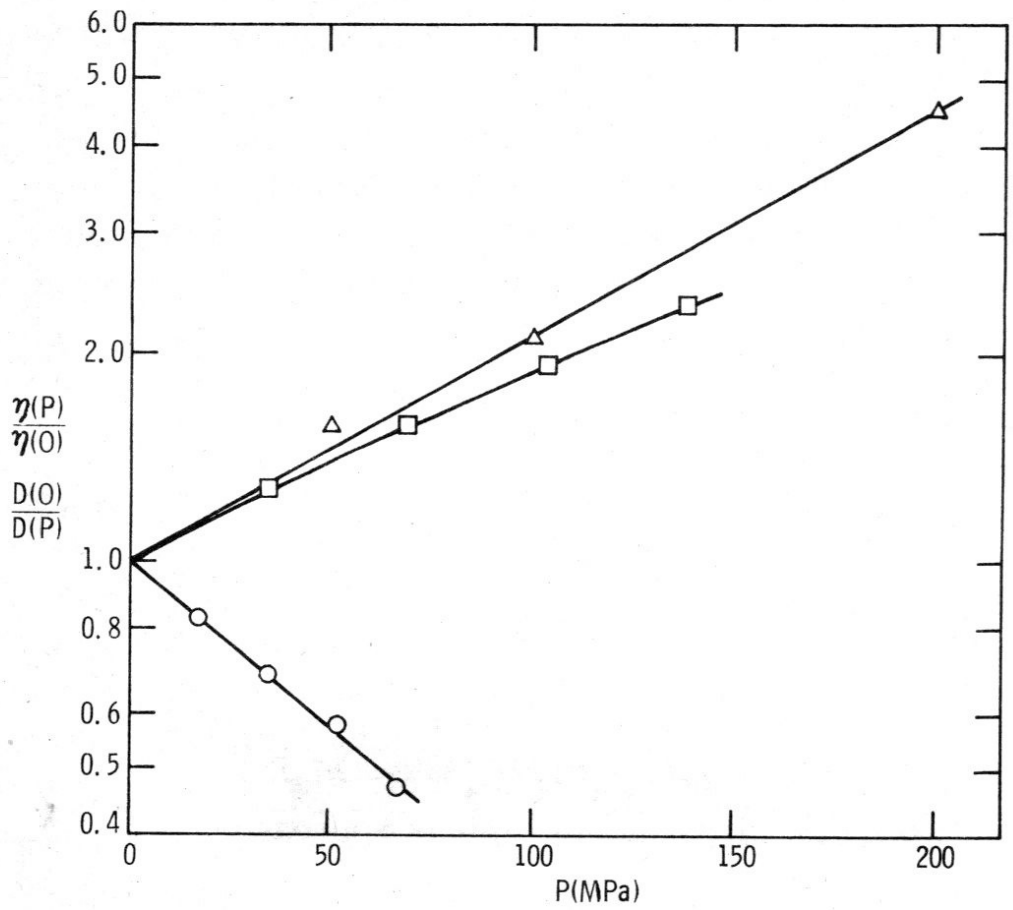

FIG. 1. The pressure dependence of the viscosity[6] (△) and the diffusion constant of octane compressed by helium (□) and argon (○).

II. EXPERIMENTAL

A. Instrumentation

The NMR relaxation measurements were performed on a Bruker SXP wideband spectrometer with a Varian V-3800-1 high resolution magnet. Operating frequencies were 90 and 14 MHz for the hydrogen and deuterium nuclei, respectively.

The pressure vessel was constructed of a beryllium-copper alloy, Berylco-25. Inside this vessel, the octane

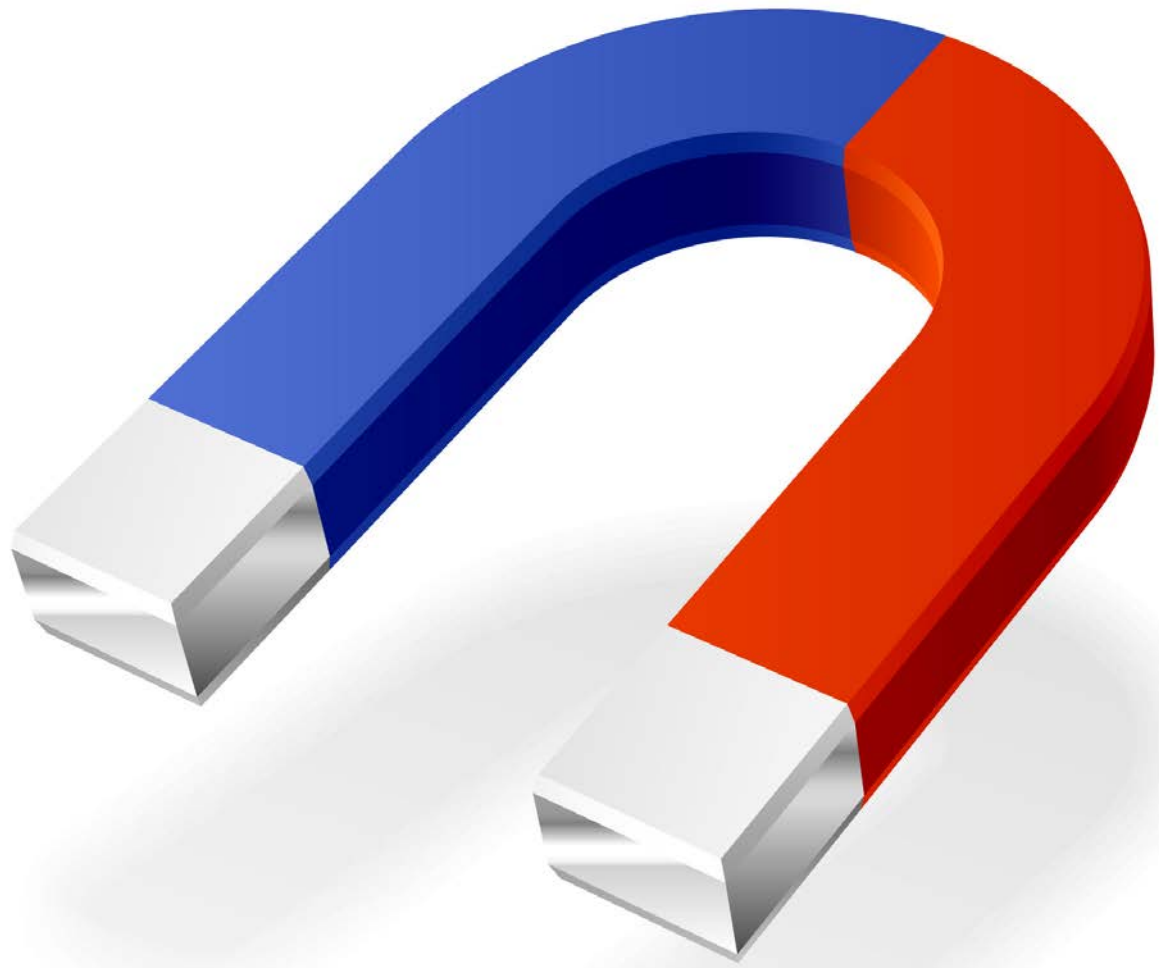

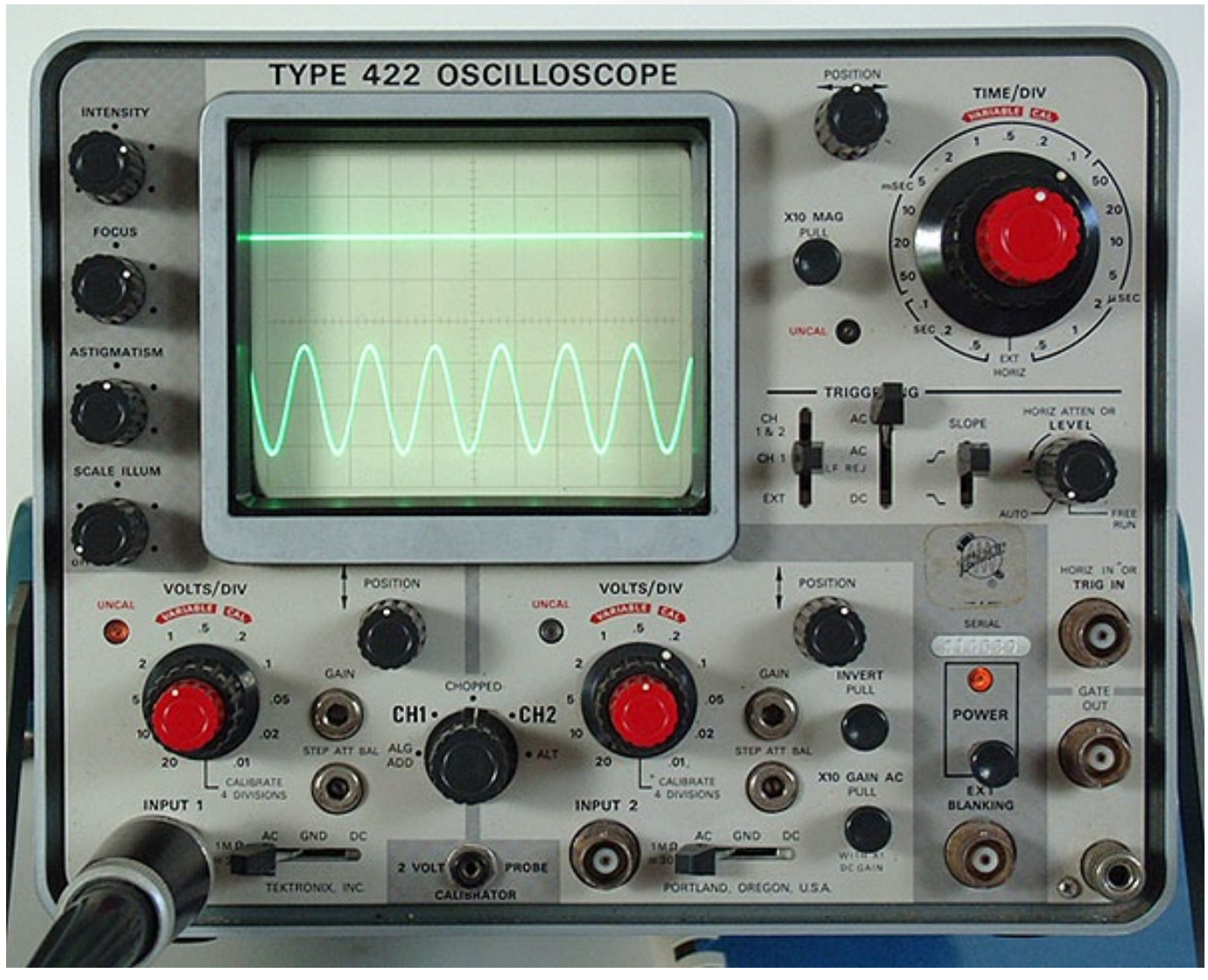
TYPE 422 OSCILLOSCOPE
INTENSITY
FOCUS
ASTIGMATISM
SCALE ILLUM
POSITION
TIME/DIV
X10 MAG
PULL
UNCAL
SLOPE
LEVEL
AUTO
FREE RUN
VOLTS/DIV
GAIN
STEP ATT BAL
CHOPPED
CH1
CH2
ALT
ADD
INVERT
PULL
X10 GAIN AC
INPUT 1
INPUT 2
AC GND DC
2 VOLT
PROBE
CALIBRATOR
TEKTRONIX, INC.
PORTLAND, OREGON, U.S.A.
SERIAL
POWER
EXT
BLANKING
TRIG IN
GATE
OUT

Domain Structure in Polyurethanes

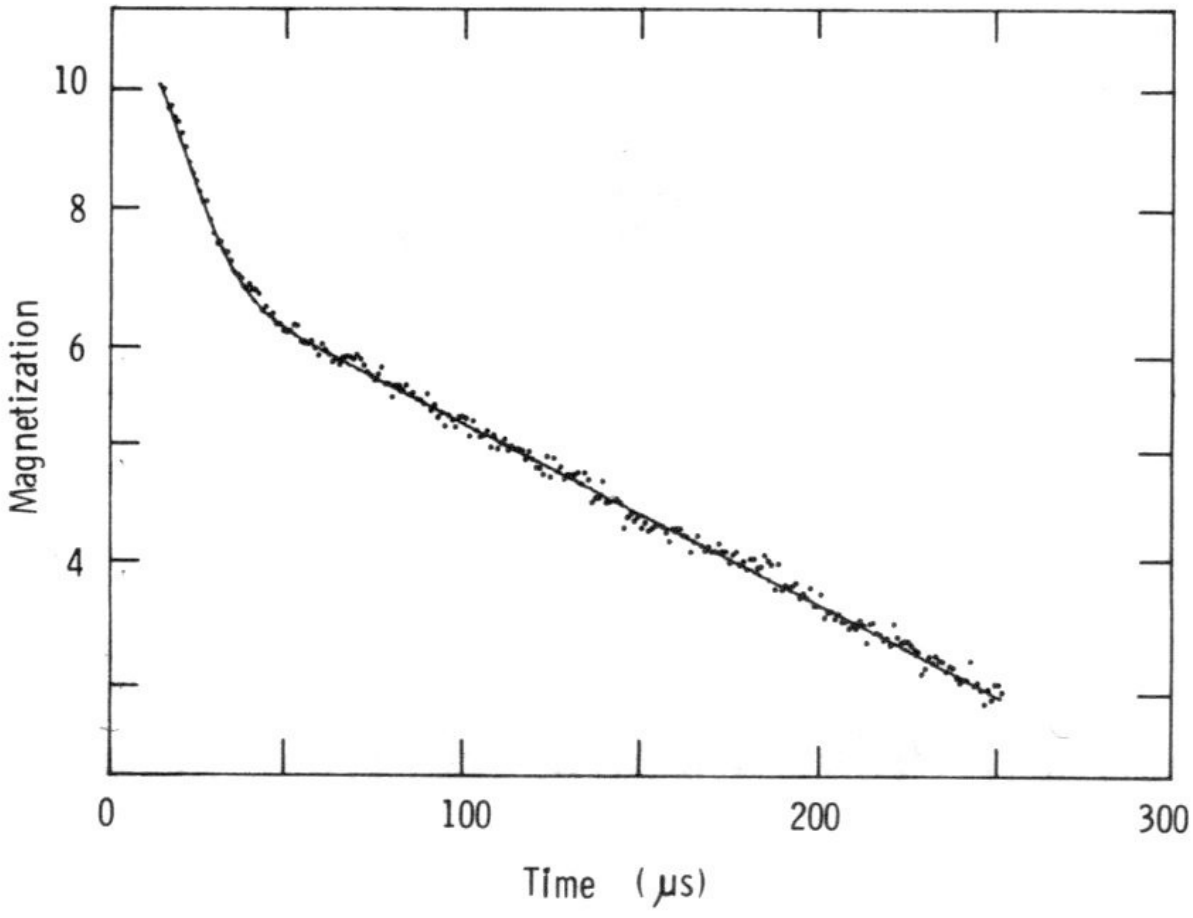

Spin Diffusion between Microphases

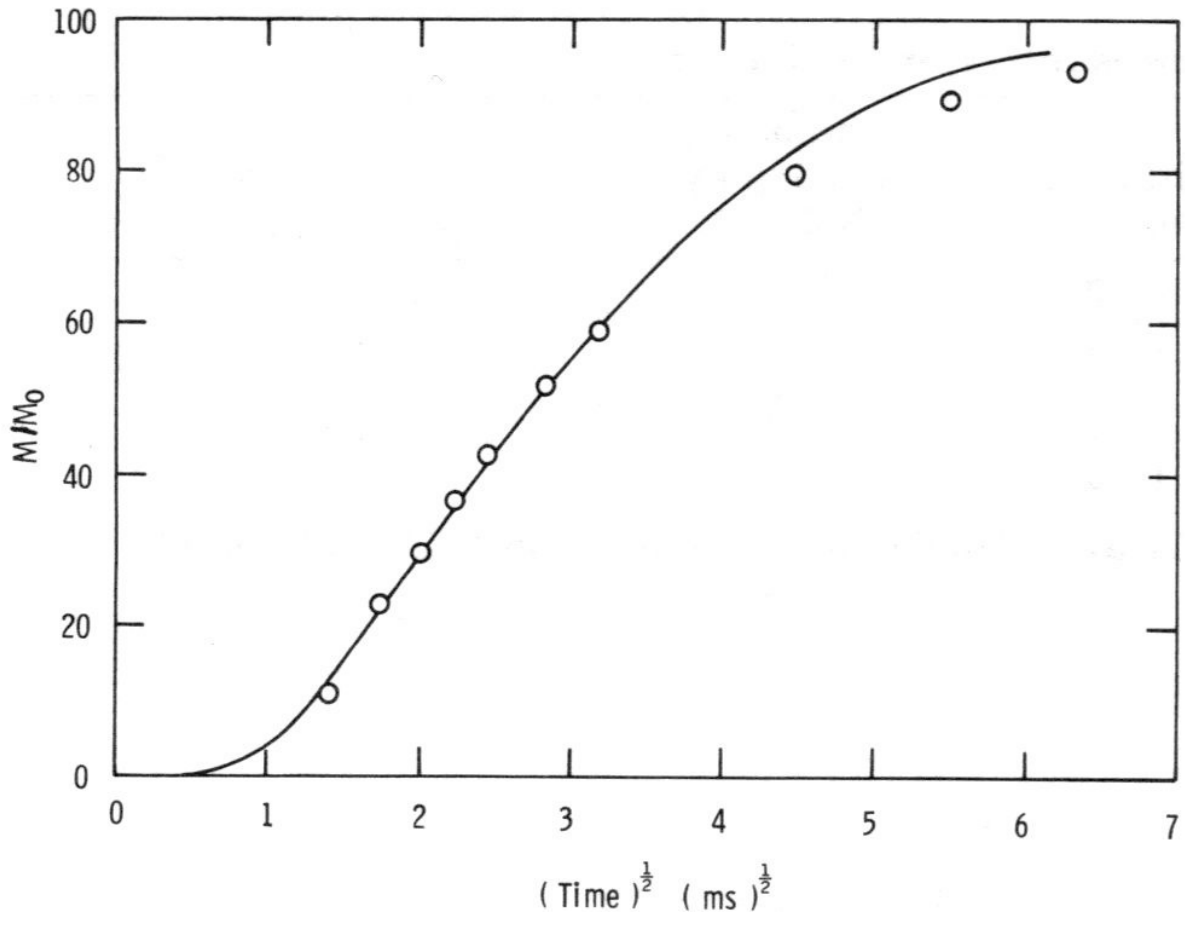

Biomation 610
Transient Recorder

Fabritek (Nicolet) 1072
Digital Recorder

DEC PDP 11/10
with Lab Interface

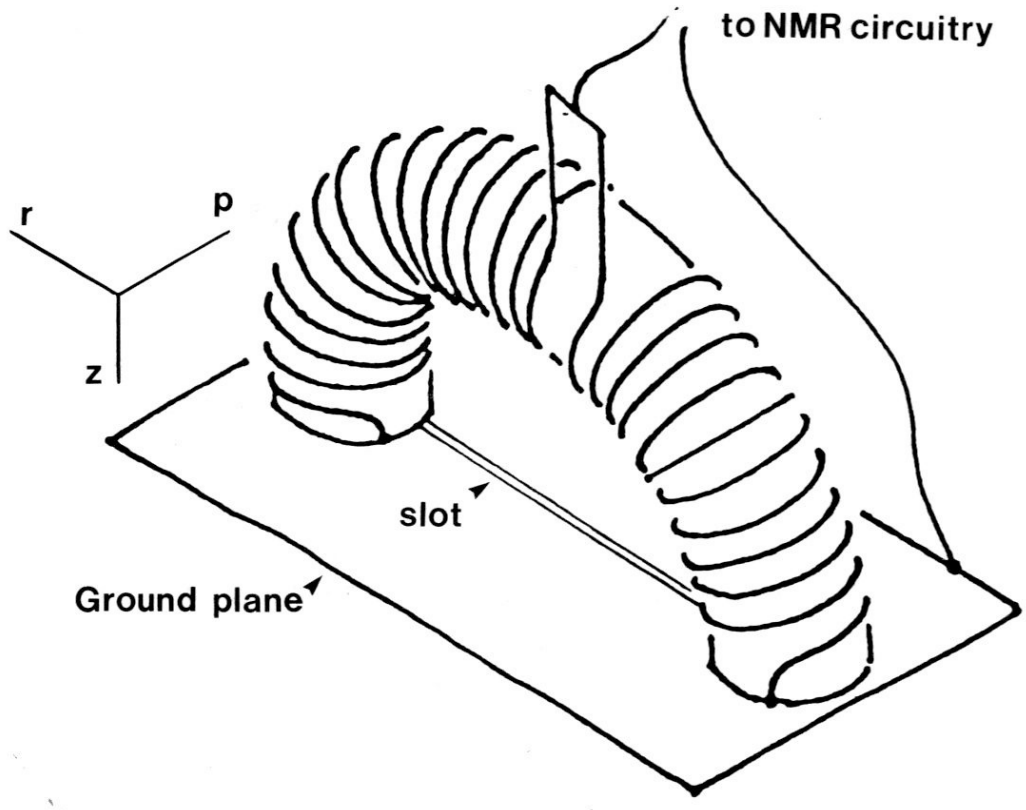

FIG. 1. A sketch of the semitoroidal coil showing the oppositely wound sections connected in parallel and the necessary slot in the ground plane. A coordinate frame labeling scheme is also shown.

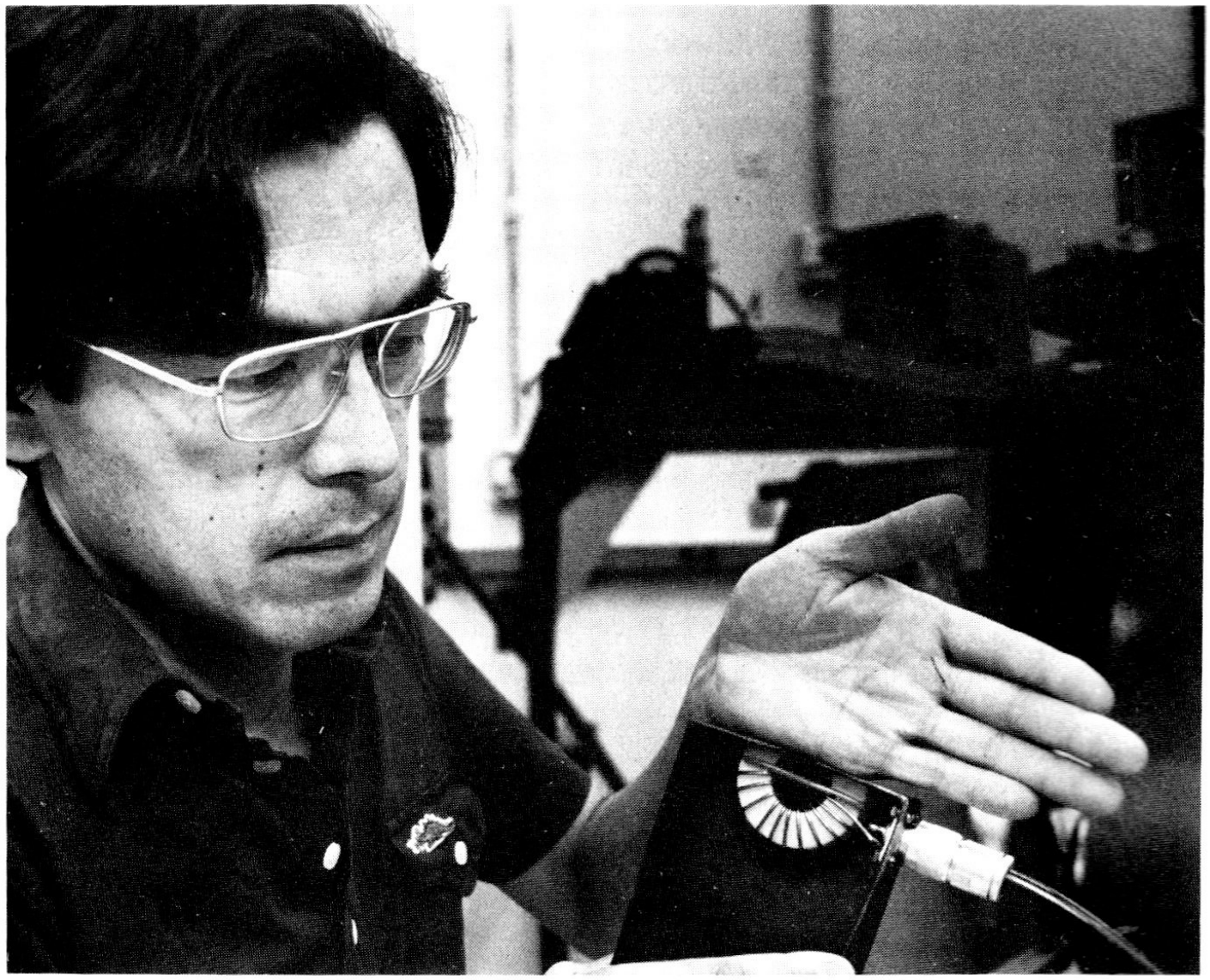

E. Fukushima of Los Alamos National Laboratory holds model of coil that enhances remote sensing capability of NMR devices.

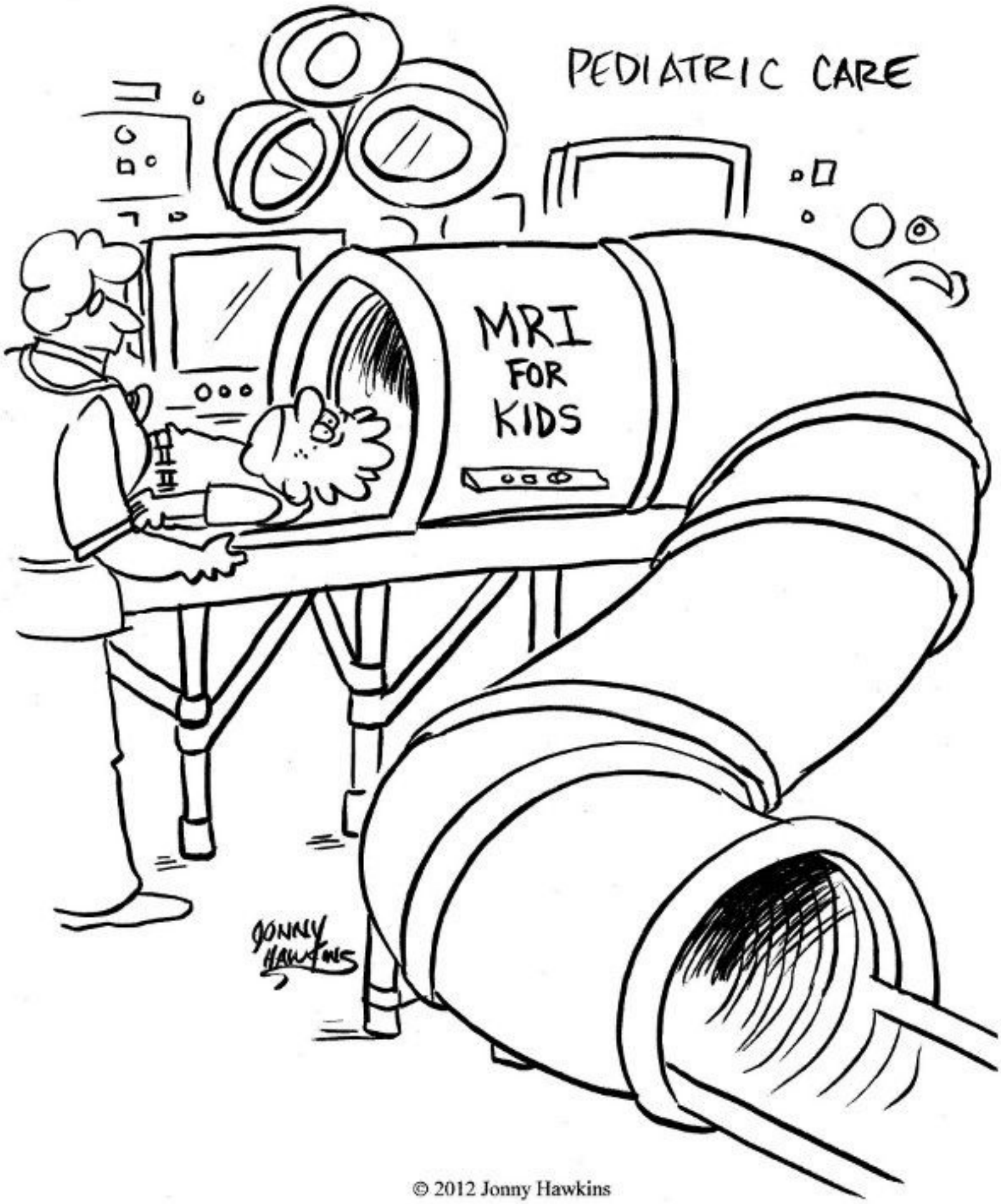

^{29}Si nuclear magnetic resonance study of plasma-polymerized* hexamethyldisiloxane[a)]

R. A. Assink, A. K. Hays, and R. W. Bild
Sandia National Laboratories, Albuquerque, New Mexico 87185

B. L. Hawkins
Colorado State University, Fort Collins, Colorado 80523

(Received 29 April 1985; accepted 16 May 1985)

angle spinning and cross-polarization techniques (MAS/CP). ^{29}Si NMR is expected to be a sensitive probe of the film structure since the siloxane moiety

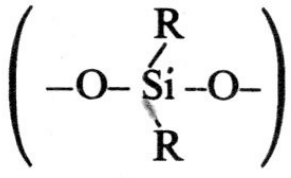

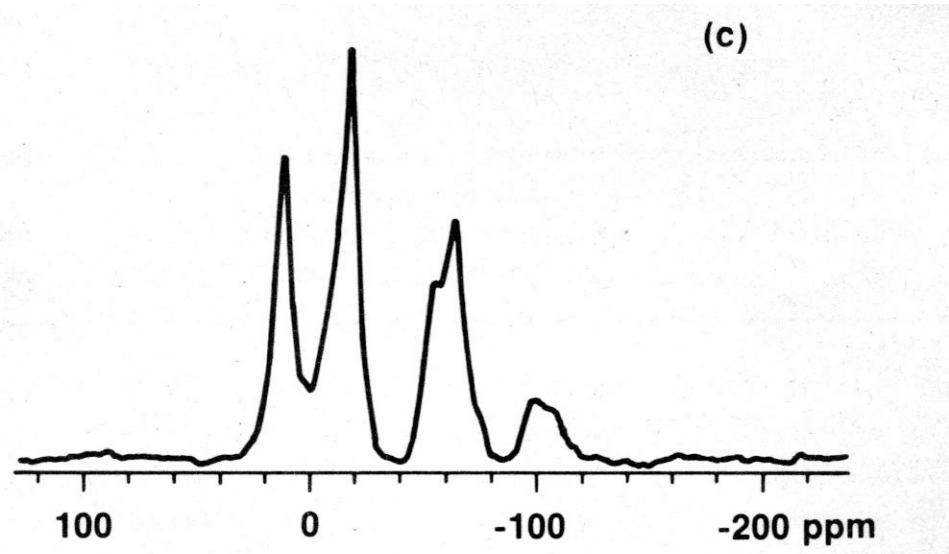

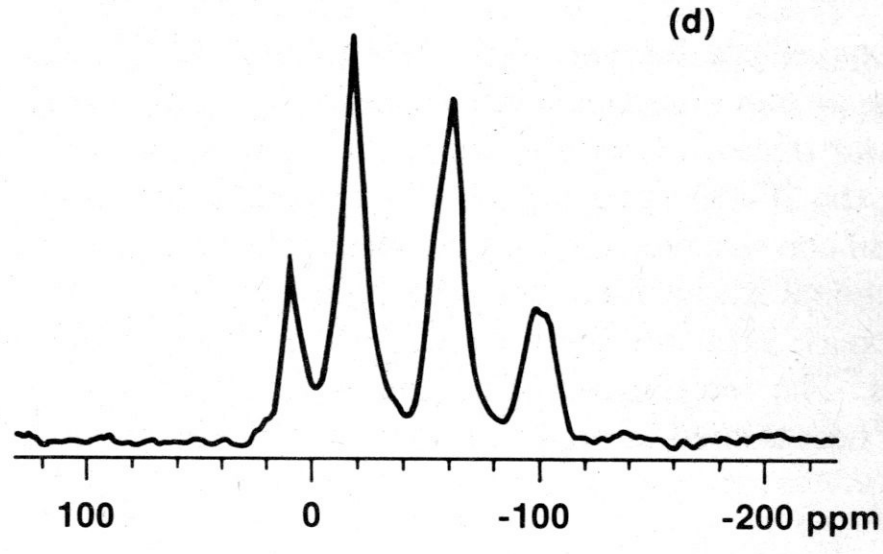

Sol-Gel Structure and Kinetics

Bruce Kay, Jeff Brinker

$Si\text{-}(OCH_3)_4$

$$SiOR + H_2O \rightarrow SiOH + ROH \quad (1)$$

$$SiOH + SiOH \rightarrow Si\text{-}O\text{-}Si + H_2O \quad (2)$$

$$SiOR + SiOH \rightarrow Si\text{-}O\text{-}Si + ROH \quad (3)$$

The ^{29}Si spectra were recorded at 39.6 MHz on a Chemagnetics console interfaced to a General Electric 1280 data station and pulse programmer. The silicon-free probe and 20 mm polytrifluorochloroethylene sample tubes were purchased from Cryomagnetics. The 4.7 T wide bore magnet was constructed by Nalorac Cryogenics. From 4 (during the early stages of the reaction) to 64

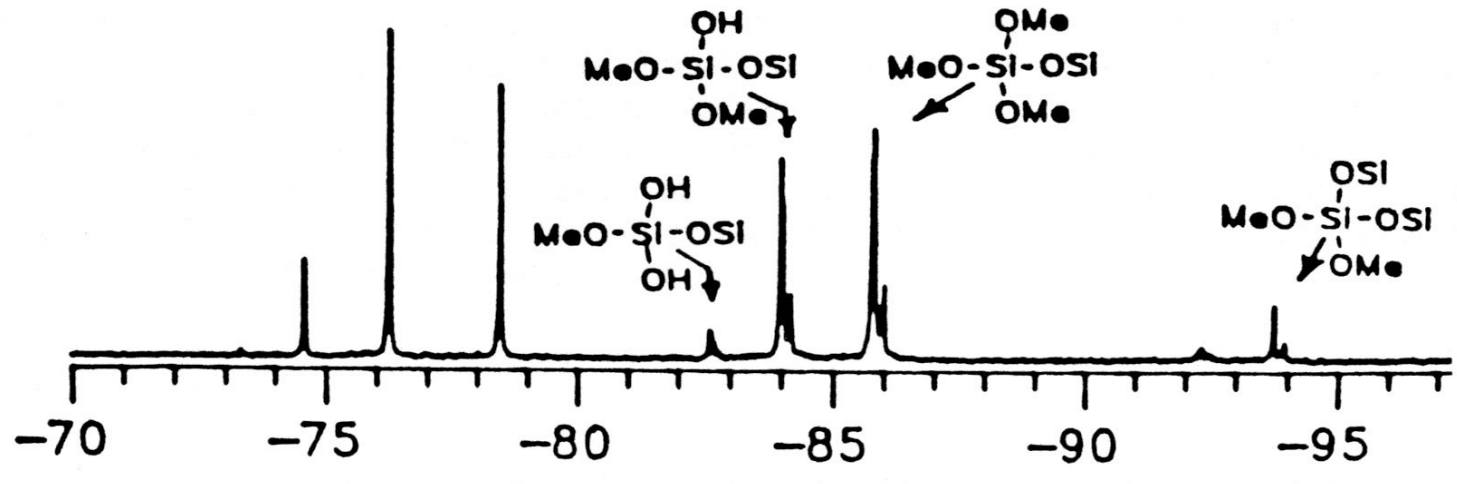

Figure 3. The ^{29}Si NMR spectrum of an acid-catalyzed tetramethoxysilane (TMOS) sol-gel which has reacted for 1 hour.

Fig. 1. The initial condensation rates divided by the initial silanol concentration versus the initial silanol concentration. This plot should be linear with a slope of $k_{CW} - k_{CA}$ and an intercept of $k_{CA}\,[SiOR]_0$.

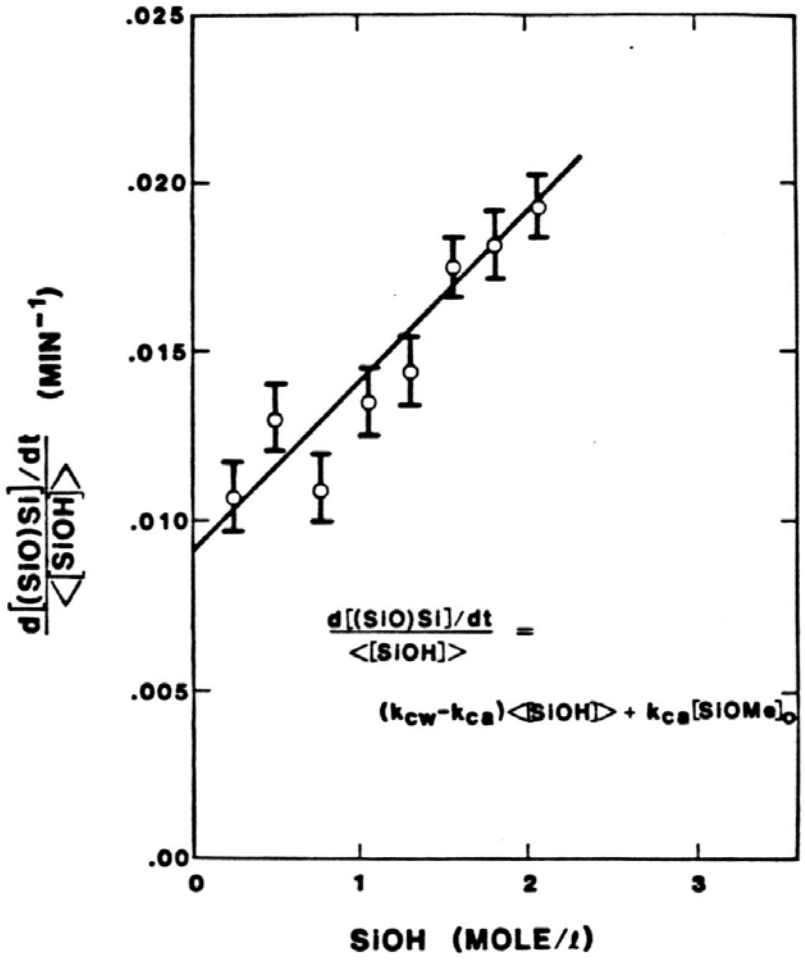

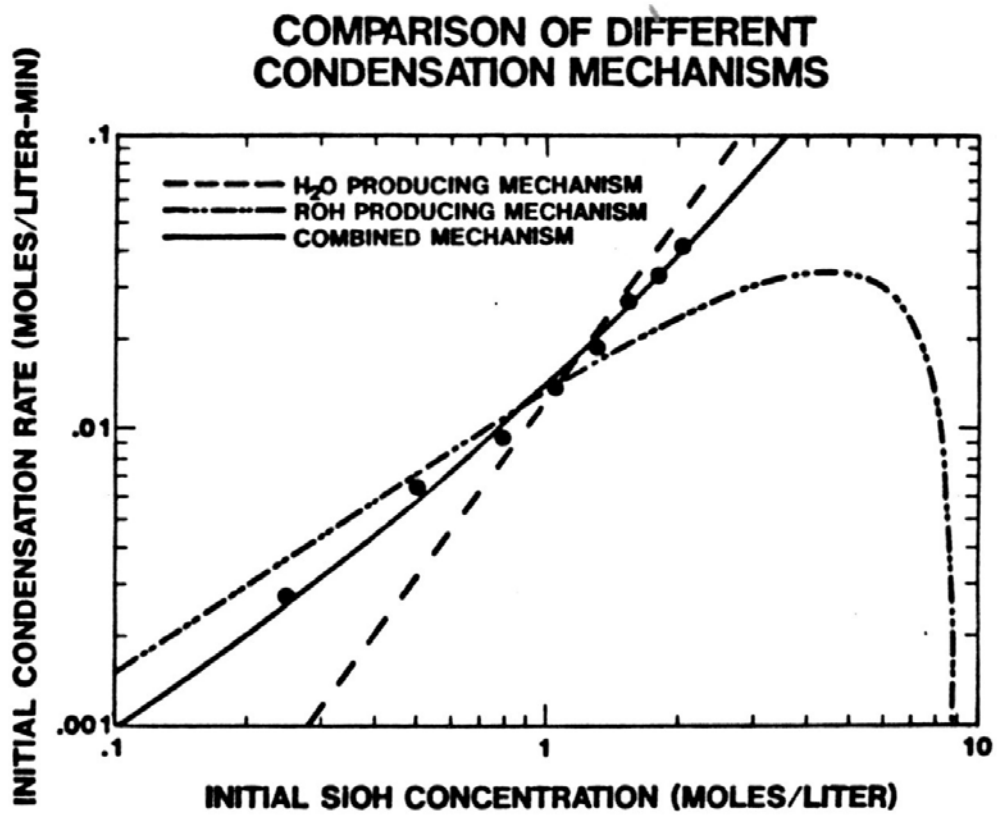

The dependence of the initial overall condensation rate on the initial silanol concentration for the various condensation mechanisms. The experimental results are also shown.

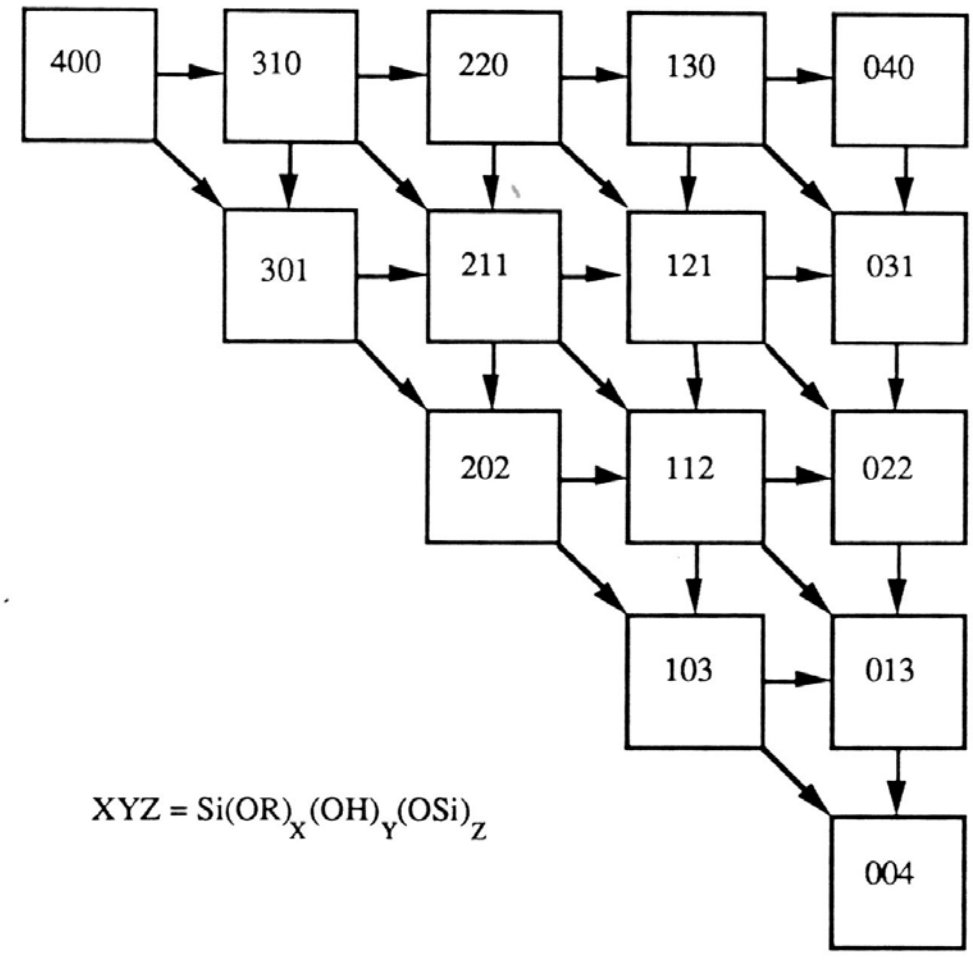

Figure 1. The 15 possible nearest neighbor functional group distributions in a silicate sol-gel.

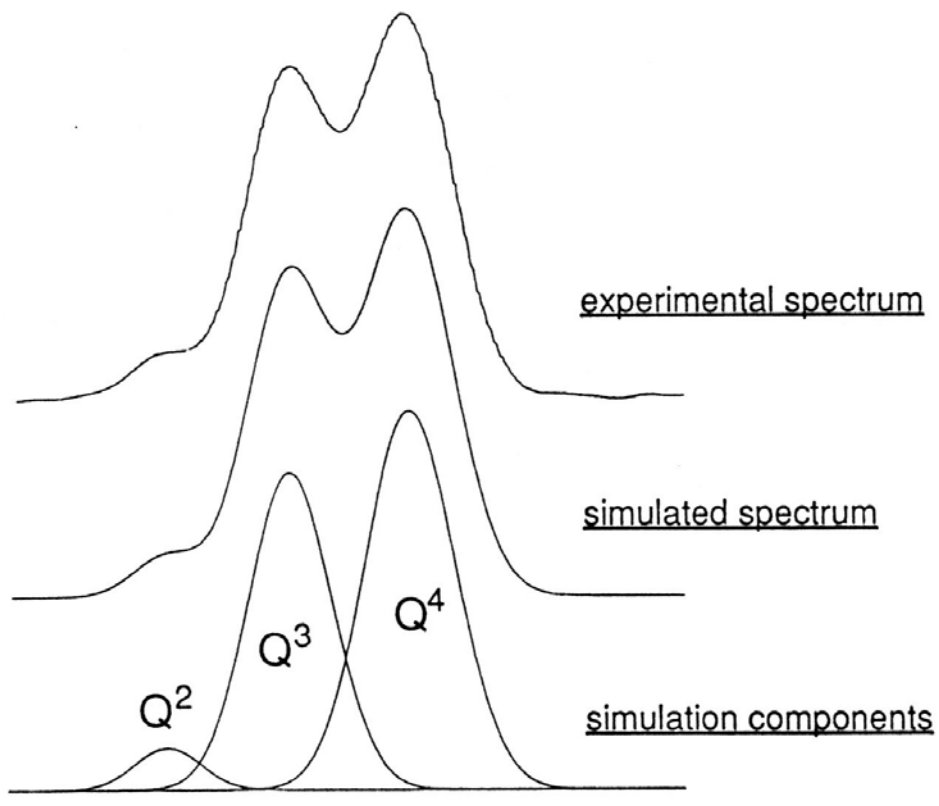

Figure 4. The ^{29}Si NMR spectrum of an ammonia catalyzed TEOS sol-gel reacted for 24 hours.

"Therefore, we can draw the conclusion that long-term exposure to high magnetic fields has no known harmful physical effect."

Density Profiles of a Draining Foam by Nuclear Magnetic Resonance Imaging

R. A. Assink
Sandia National Laboratories
Albuquerque, NM 87185

A. Caprihan, E. Fukushima
Lovelace Medical Foundation
Albuquerque, NM 87108

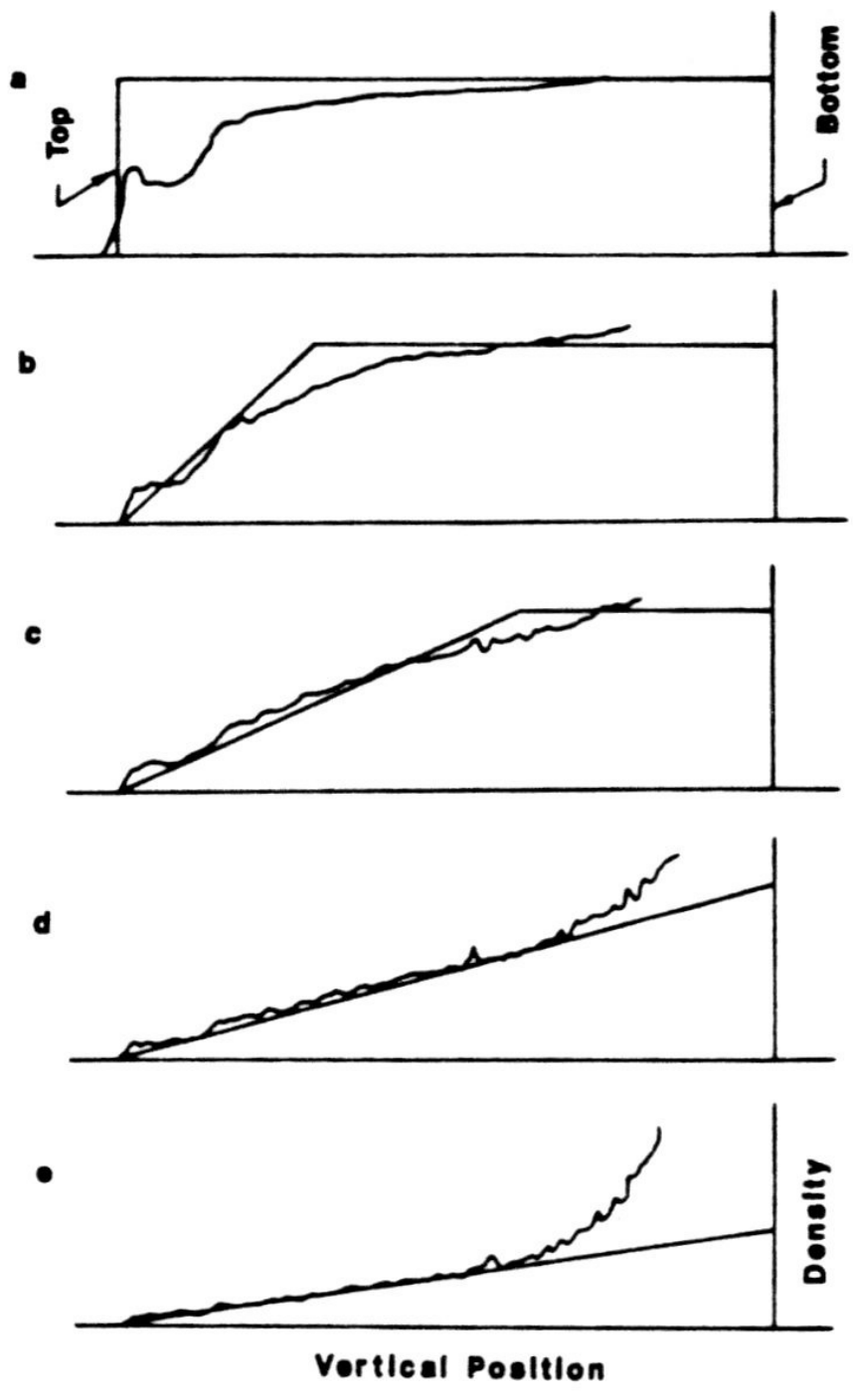

Figure 4. Experimental density profiles of a draining foam vs. those predicted by a basic foam model for drainage times of: a) 20 s; b) 15 min; c) 30 min; d) 50 min; and e) 90 min.

Power-Law Relaxation of Spin-$\frac{1}{2}$ Nuclei in Solids*

R. A. ASSINK, M. B. BOSLOUGH, AND R. T. CYGAN

Sandia National Laboratories, Albuquerque, New Mexico 87185

Received April 5, 1993; revised June 22, 1993

JOURNAL OF MAGNETIC RESONANCE, Series A **106,** 116–118 (1994)

^{29}Si MAS of a-quartz

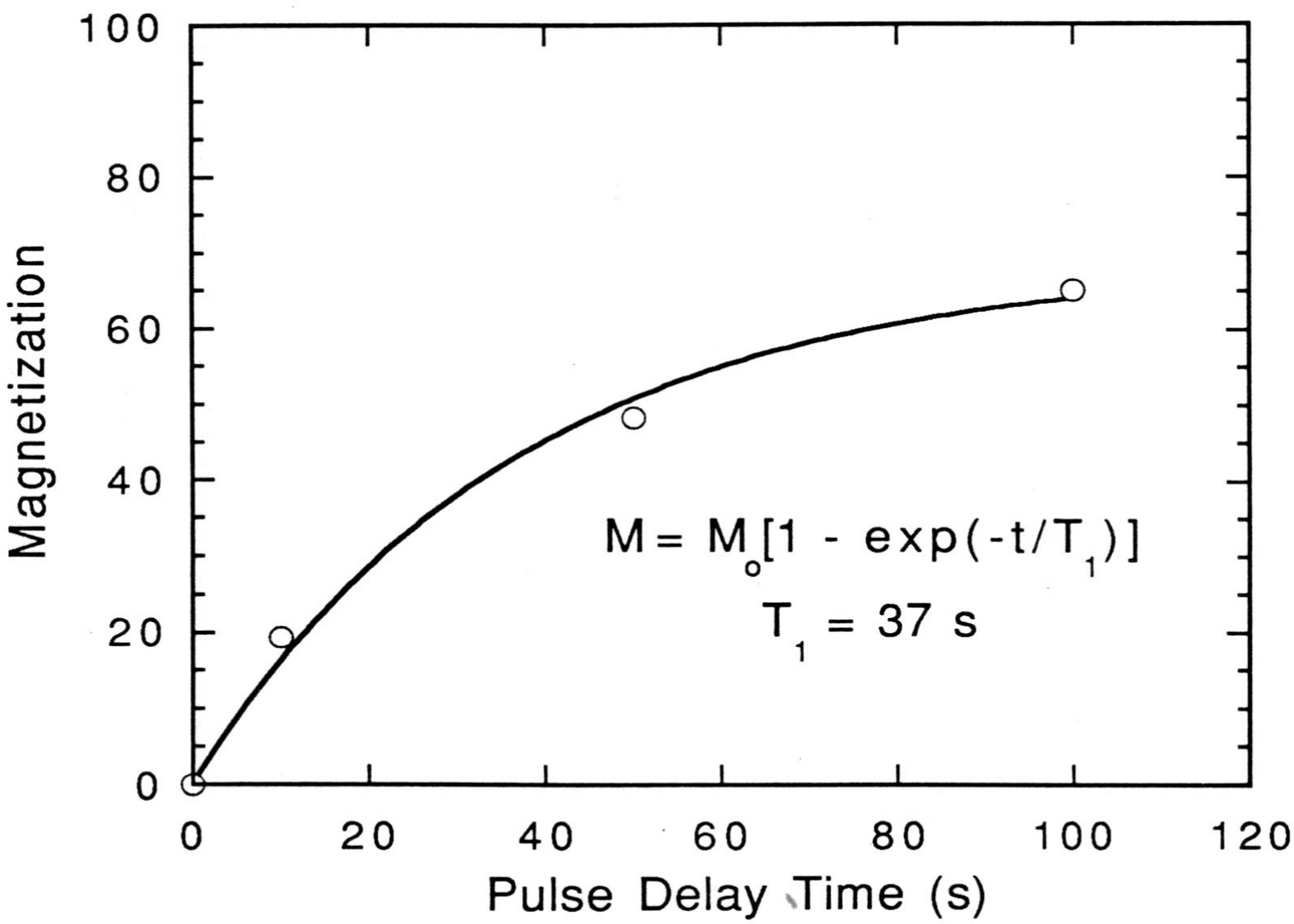

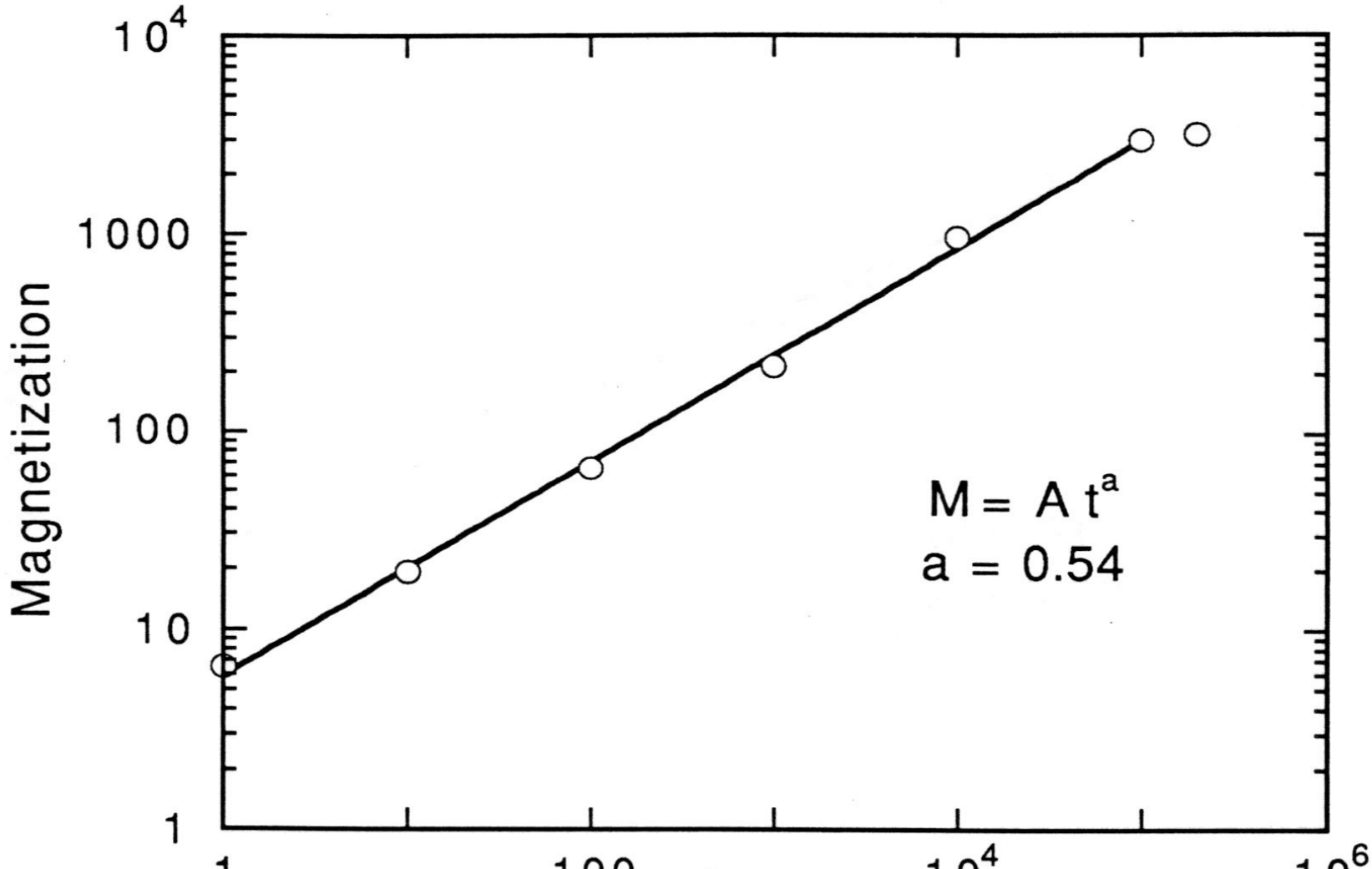

- pulse saturation sequence
- 100 s only 2% of signal
- 56 hrs, ~ quantitative
- a x 6 = dimensionality

a-quartz

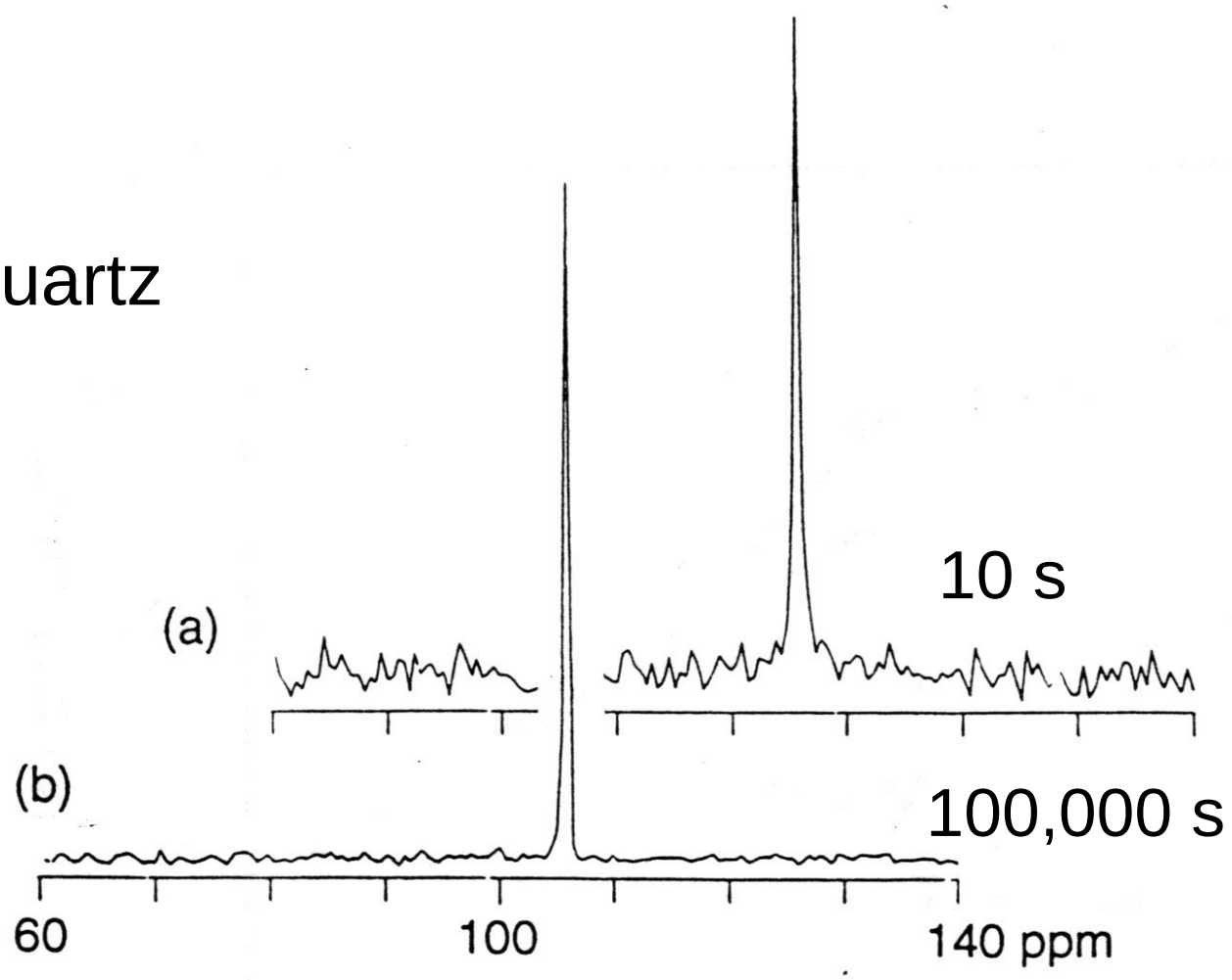

a-quartz, shocked 22 GPa

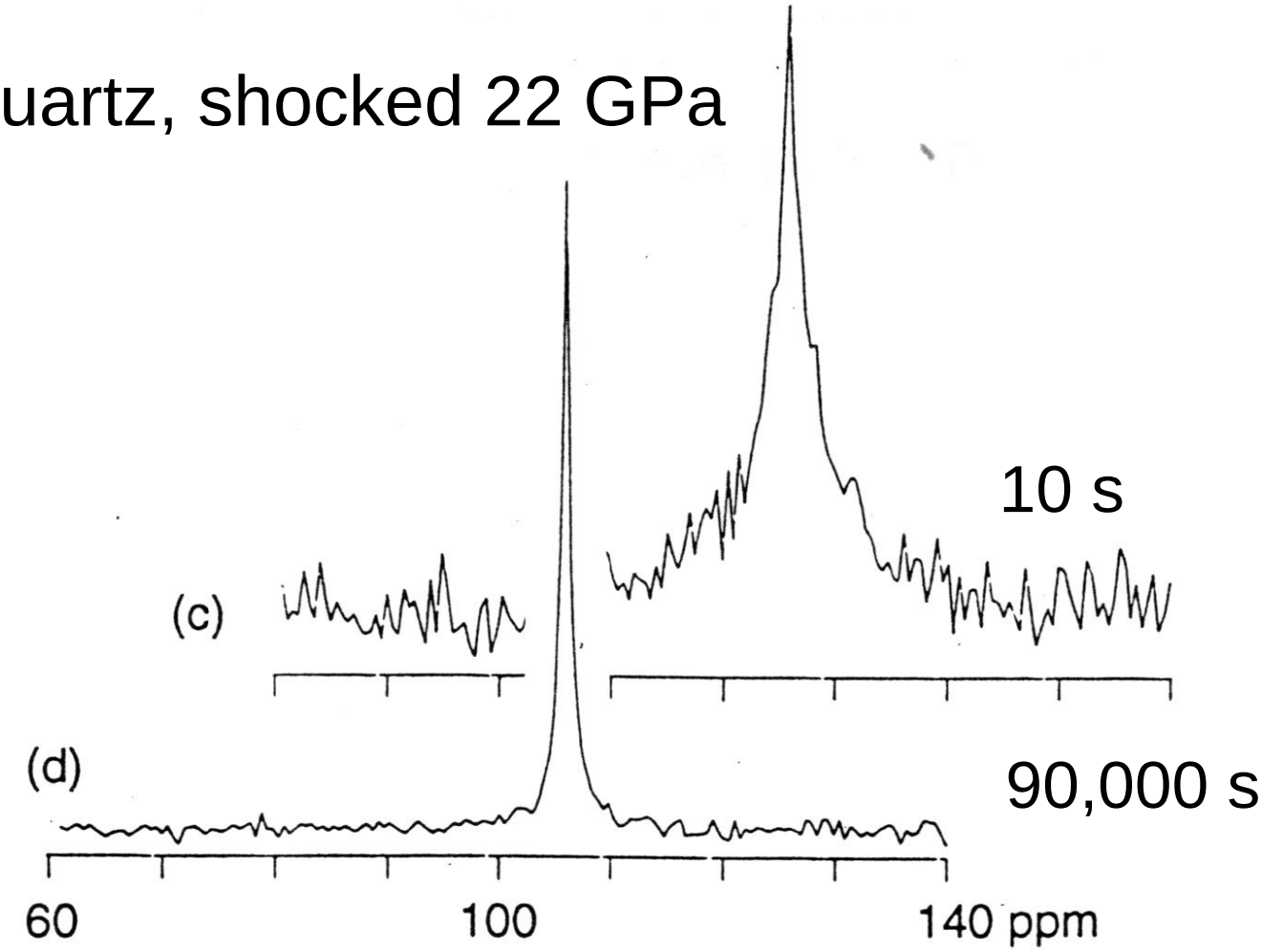

S.A. Myers · R.T. Cygan · R.A. Assink
M.B. Boslough

^{29}Si MAS NMR relaxation study of shocked Coconino Sandstone from Meteor Crater, Arizona

Phys Chem Minerals (1998) 25:313-317

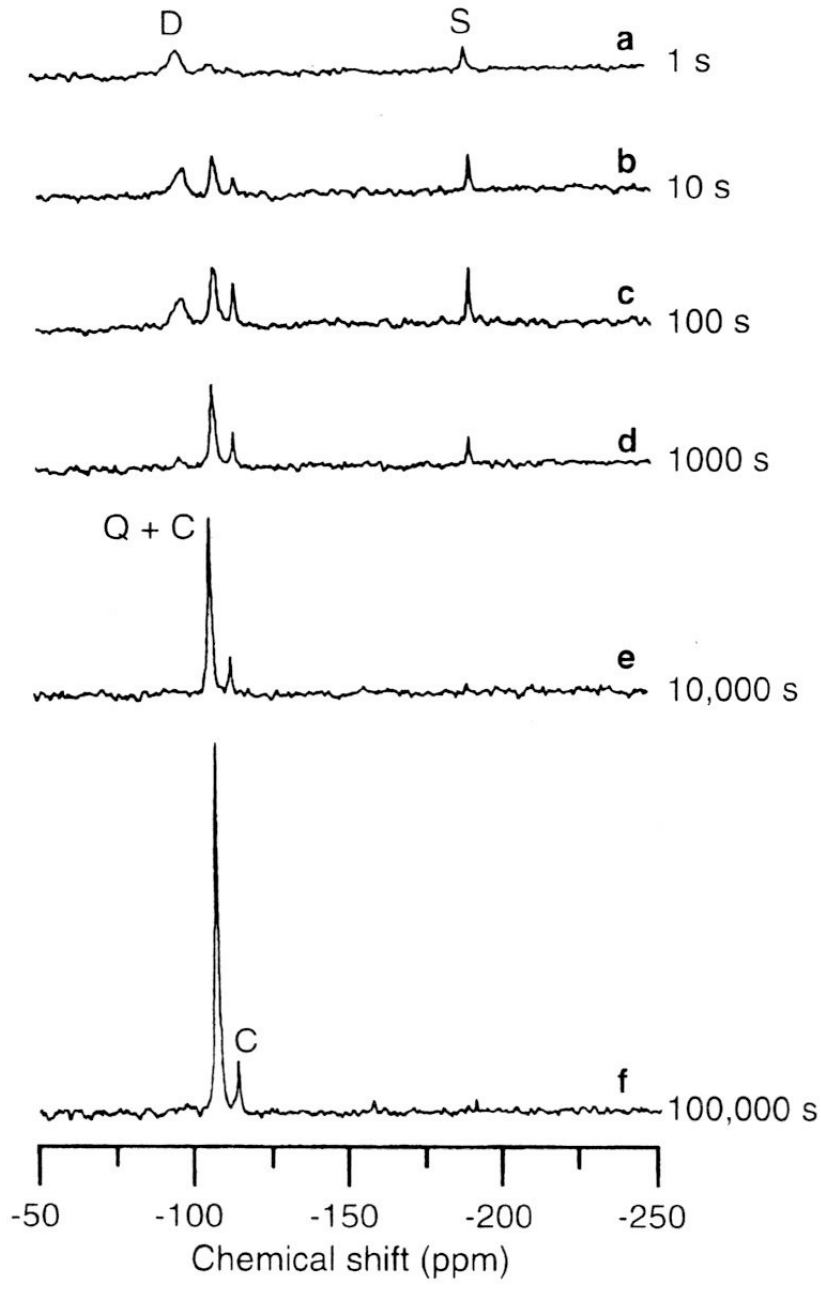

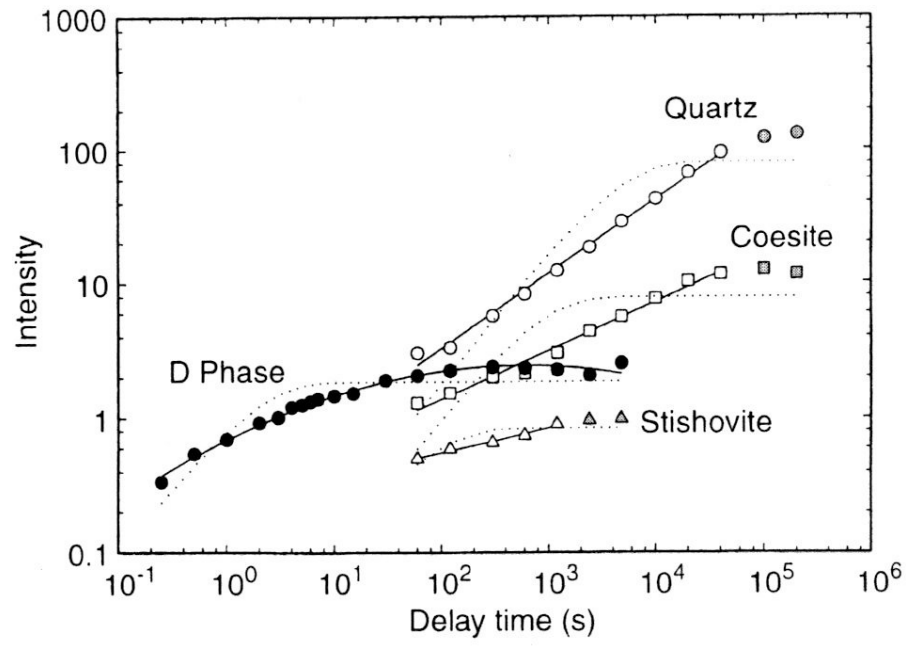

Spectra as a function of recovery time (sat. rec.)

Intercalation of molecular species into the interstitial sites of fullerene

Roger A. Assink,[a] James E. Schirber, Douglas A. Loy, Bruno Morosin, and Gary A. Carlson
Sandia National Laboratories, Albuquerque, New Mexico 87185

(Received 10 January 1992; accepted 20 April 1992)

J. Mater. Res., Vol. 7, No. 8, Aug 1992

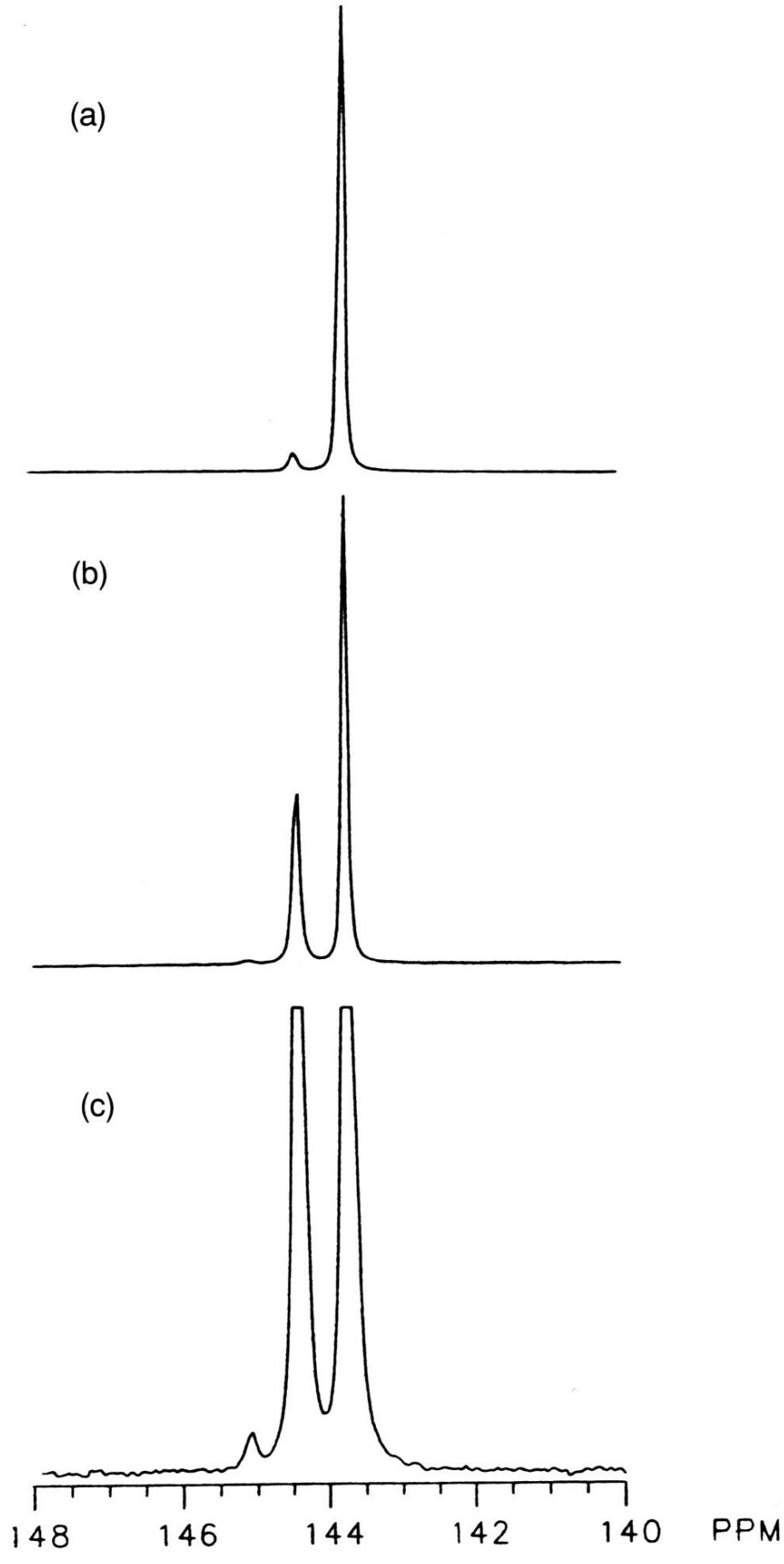

Curie's Law

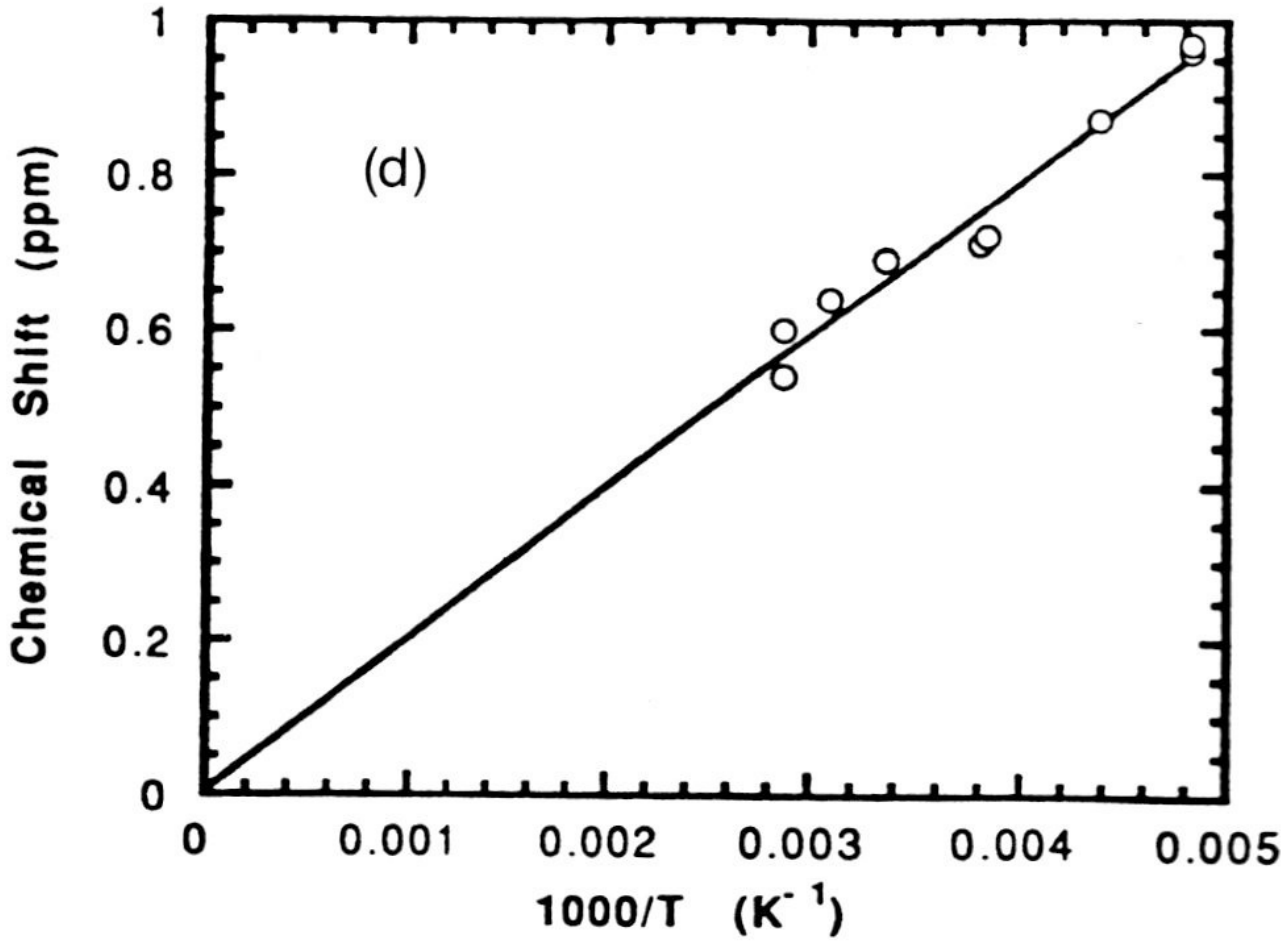

Relaxation rate ~ intensity

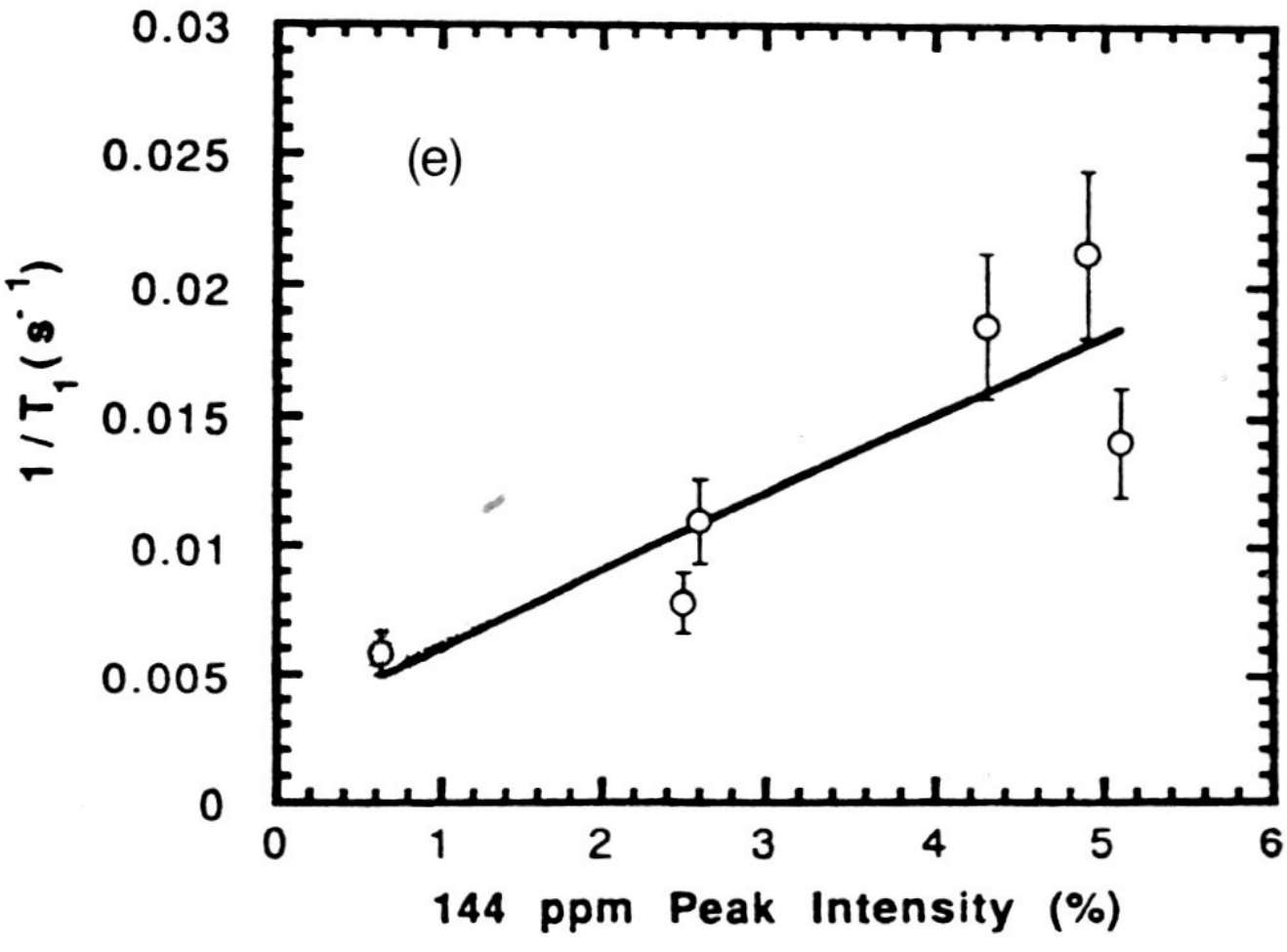

(a)

0.1 kbar oxygen

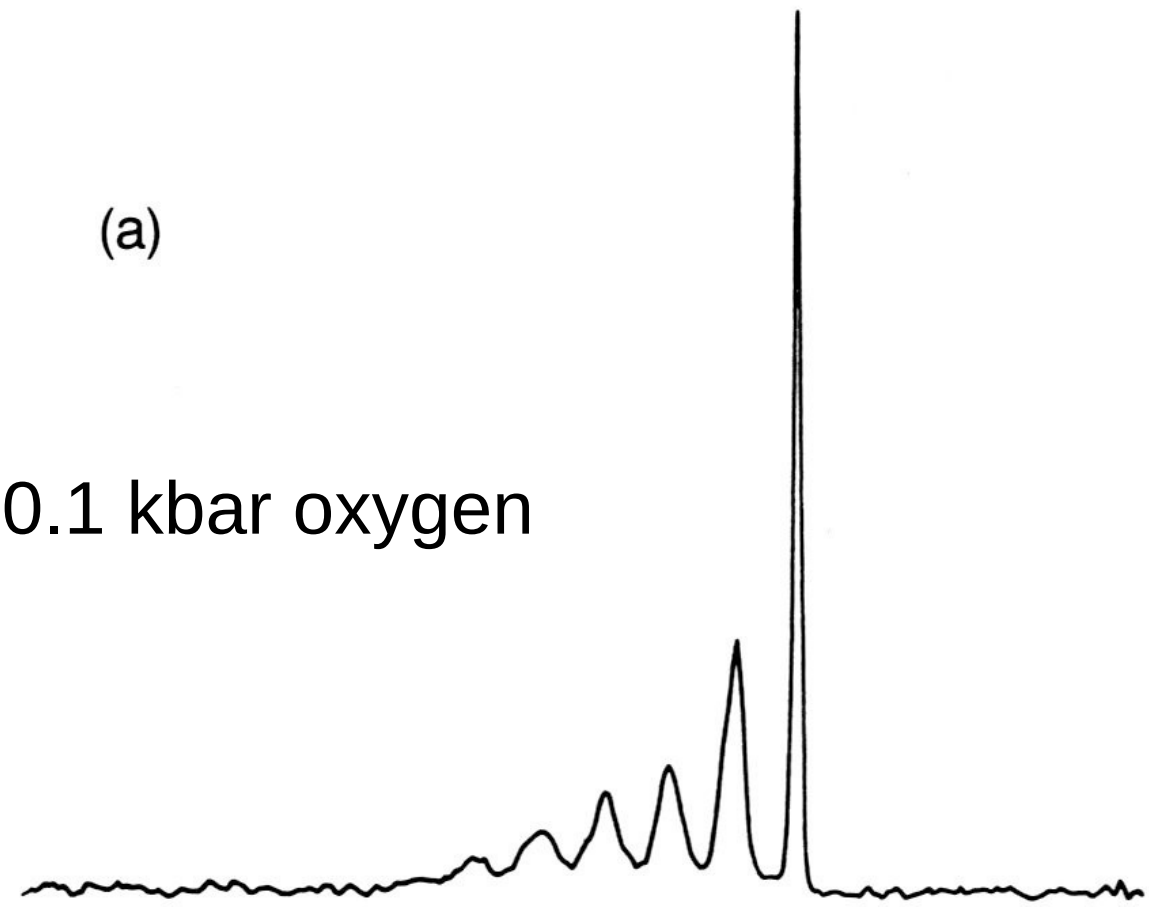

(b)

1.0 kbar oxygen

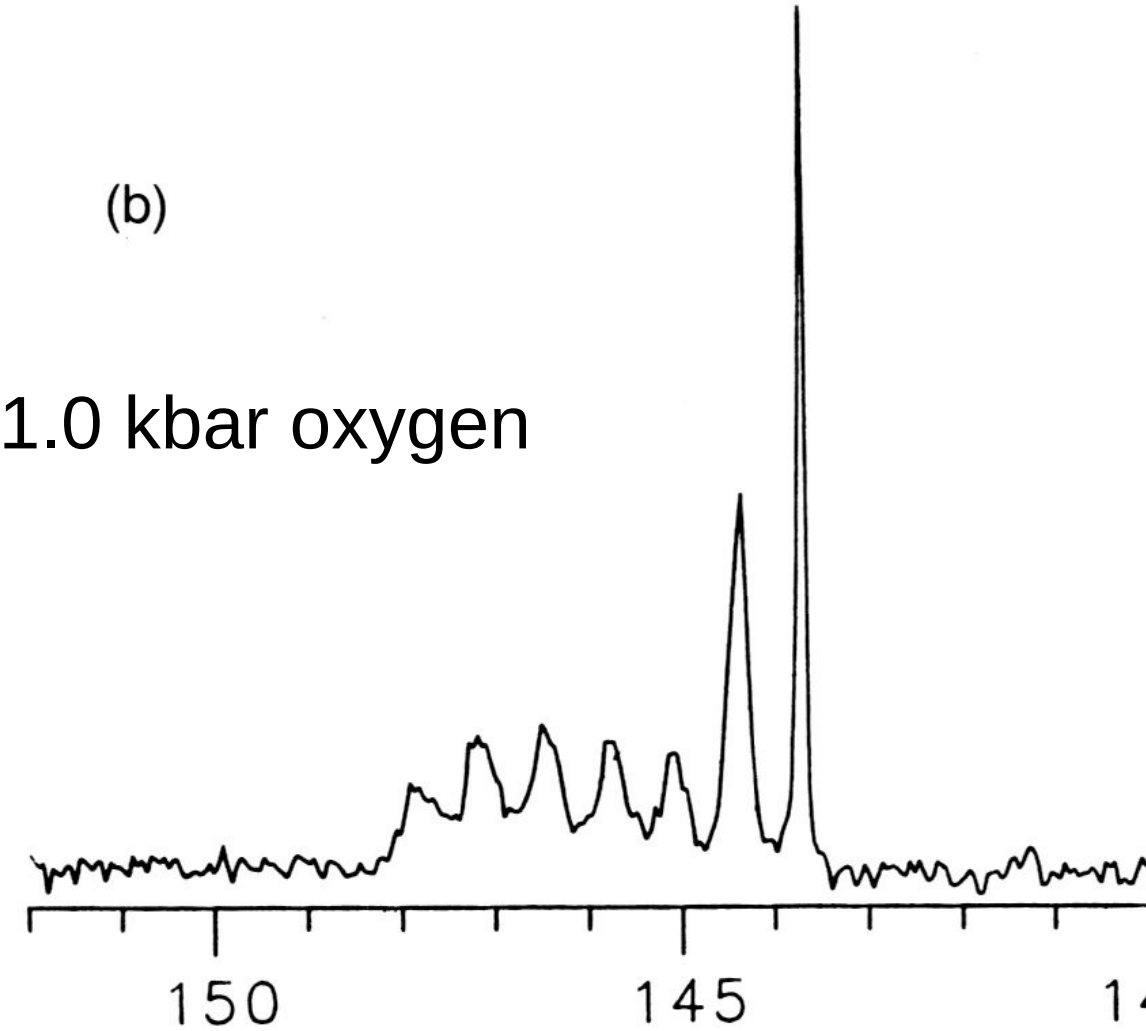

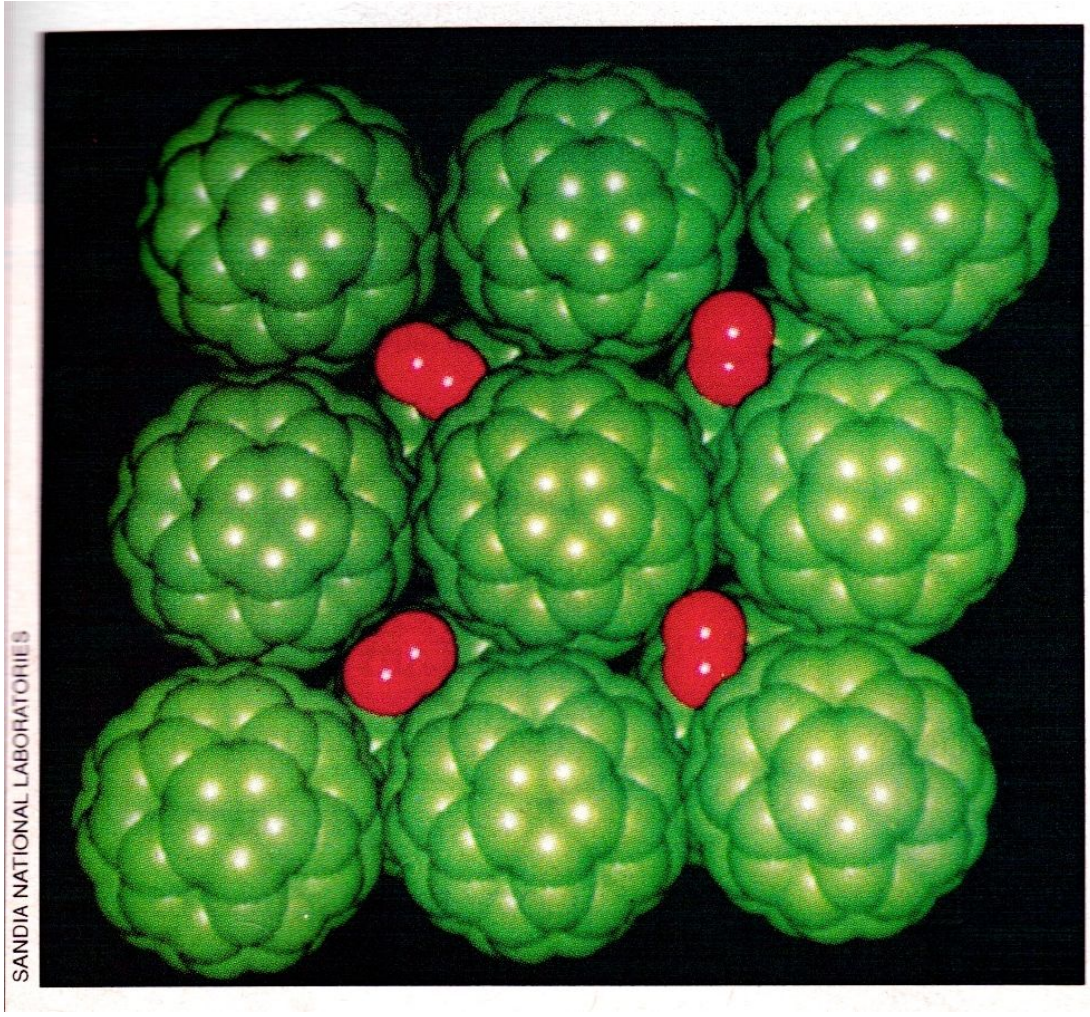

SANDIA NATIONAL LABORATORIES

need to be kept under moderate pressure to prevent leakage.

"Perhaps a more interesting application is to separate gases," he says. Hydrogen, for example, diffuses into a bucky-

Buckyball crystals might be useful for storing or separating gases. Computer graphics show a crystal in which oxygen molecules (red) are trapped in the spaces between buckyball molecules (green).

The spaces between buckminsterfullerene molecules, or "buckyballs," can accommodate molecules of oxygen or hydrogen. As a result, scientists think buckyballs could be useful in storing, releasing or separating gases.

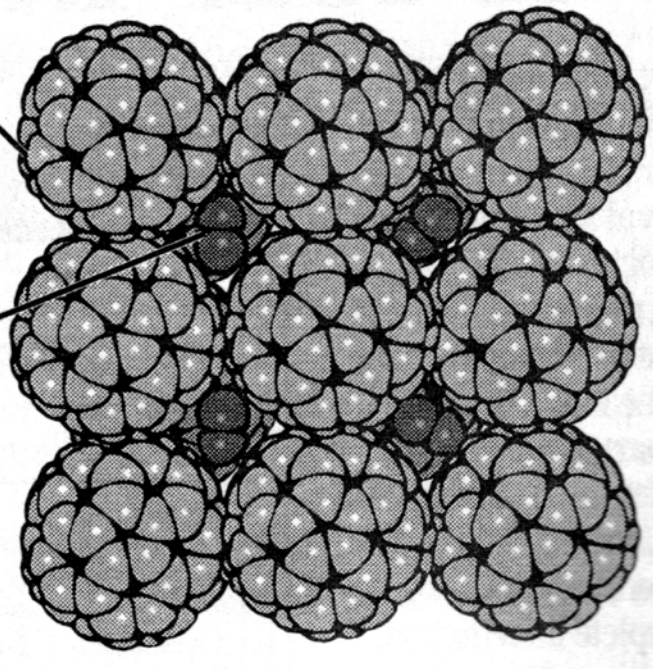

Source: Sandia National Laboratories

The New York Times

'Buckyballs' as Filters:

Researchers Give Fullerenes Gas

The Buckminsterfullerene talent show seems destined for a long run. The material's latest trick, a remarkable ability to sop up and store lots of gas molecules selectively, was revealed at Sandia National Laboratories in New Mexico, when NMR spectroscopist Roger Assink performed a routine analysis on C_{60} crystals earmarked as polymer ingredients.

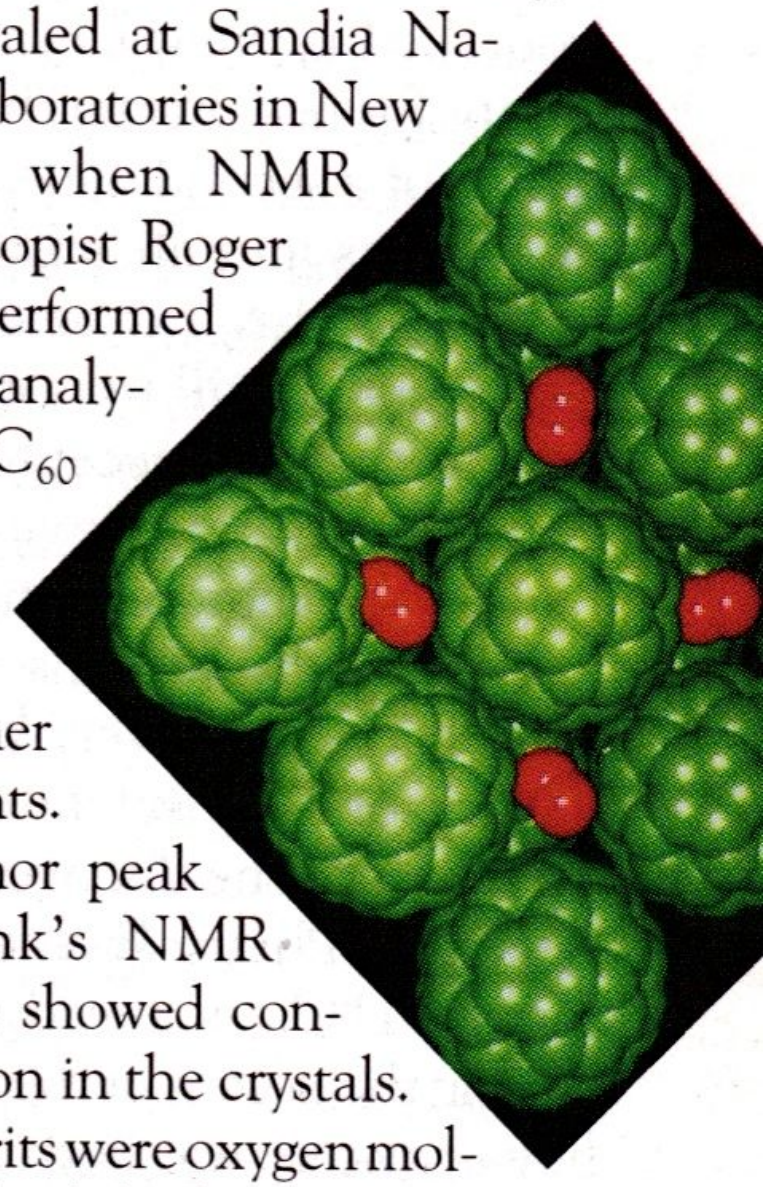

SANDIA

A minor peak in Assink's NMR spectrum showed contamination in the crystals. The culprits were oxygen molecules, which had snuggled into about 1% of the octahedral voids that form between C_{60} molecules when they pack into crystals.

Science 256, 1 May 1992, p 611

Polymer Degradation

Insulation of Control Cables in Nuclear Power Plants

- Condition Monitoring
- Degradation Mechanisms & Prediction
- Oxygen Consumption

Ken Gillen, Mat Celina, Todd Alam,
Dan Mowery, Robert Bernstein,
Roger Clough, Doug Harris

Condition Monitoring

^{1}H sensitivity ?

mg sample size

relationship to elongation

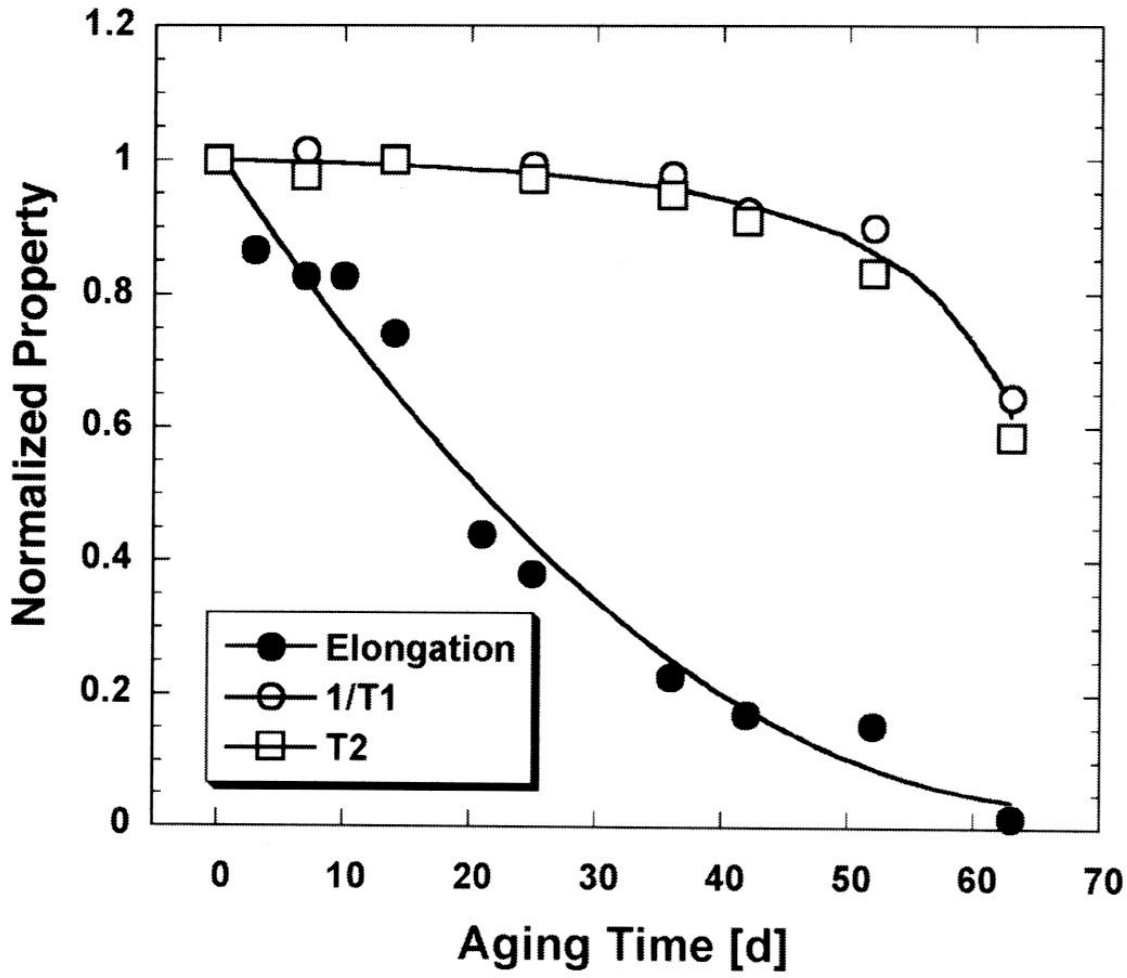

Figure 1. Normalized values of the tensile elongation and ^{1}H NMR relaxation times as a function of aging time in days at 95°C.

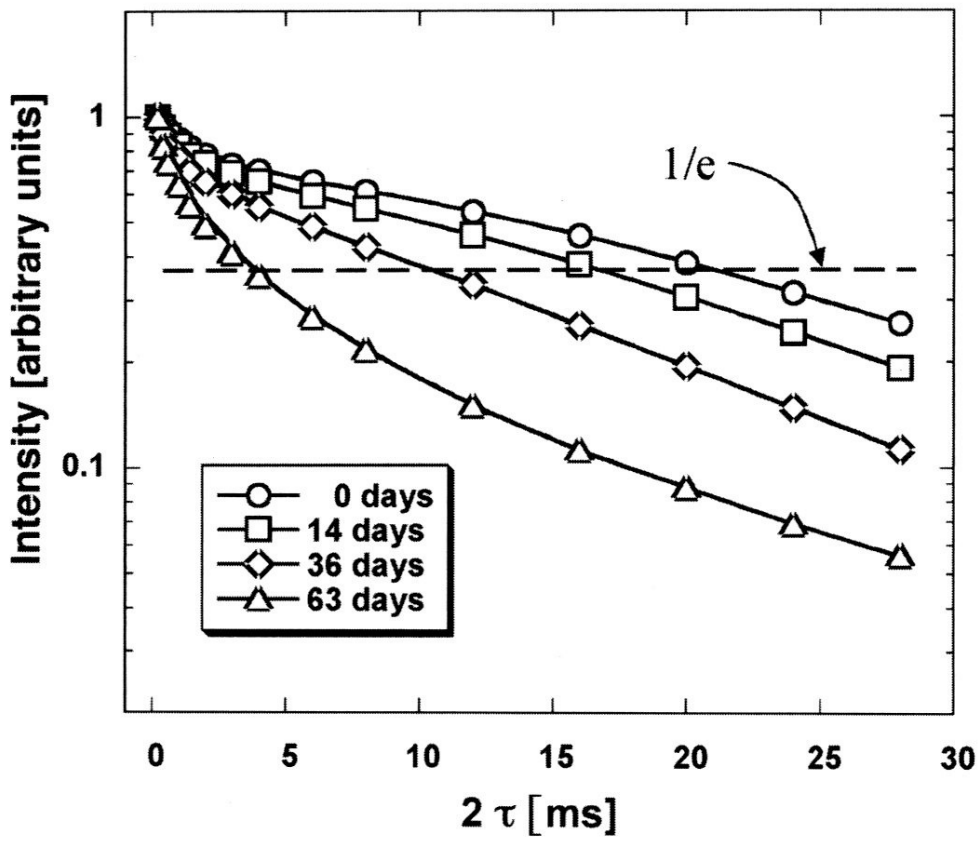

Figure 4. The ^{1}H spin-echo decay curves of unaged HTPB and HTPB aged for 14, 36, and 63 days at 95°C.

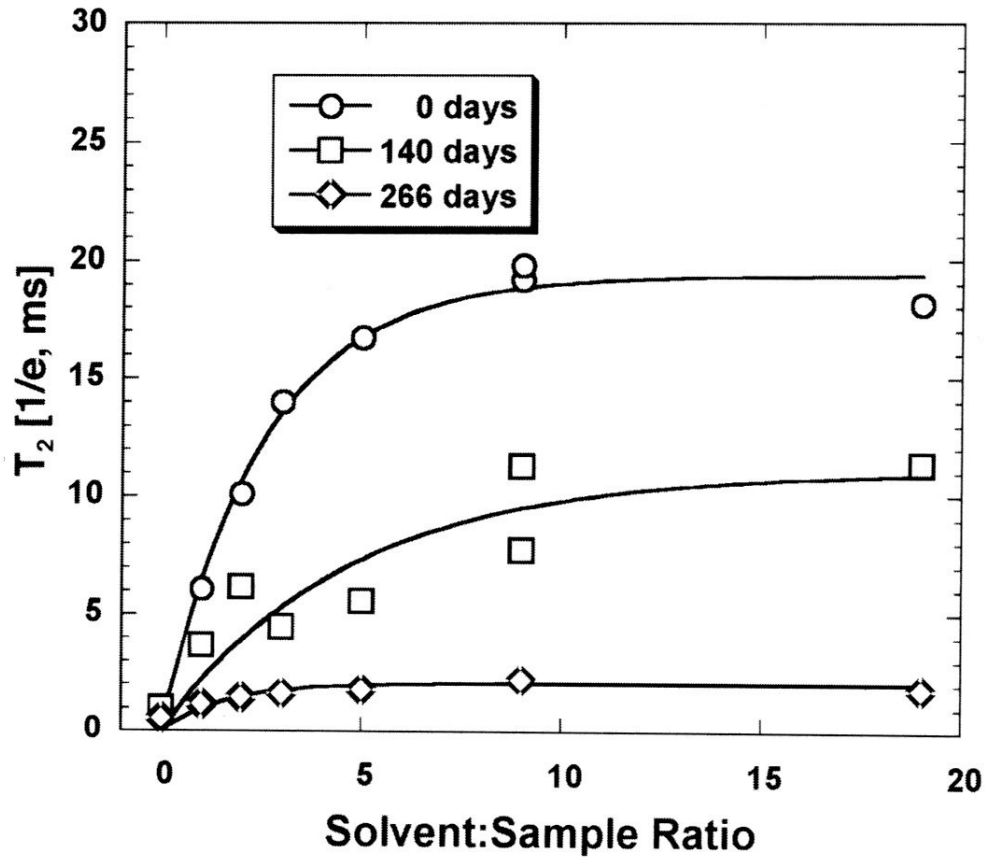

Figure 5. Dependence of the ^{1}H NMR T_2 as a function of the solvent:sample ratio.

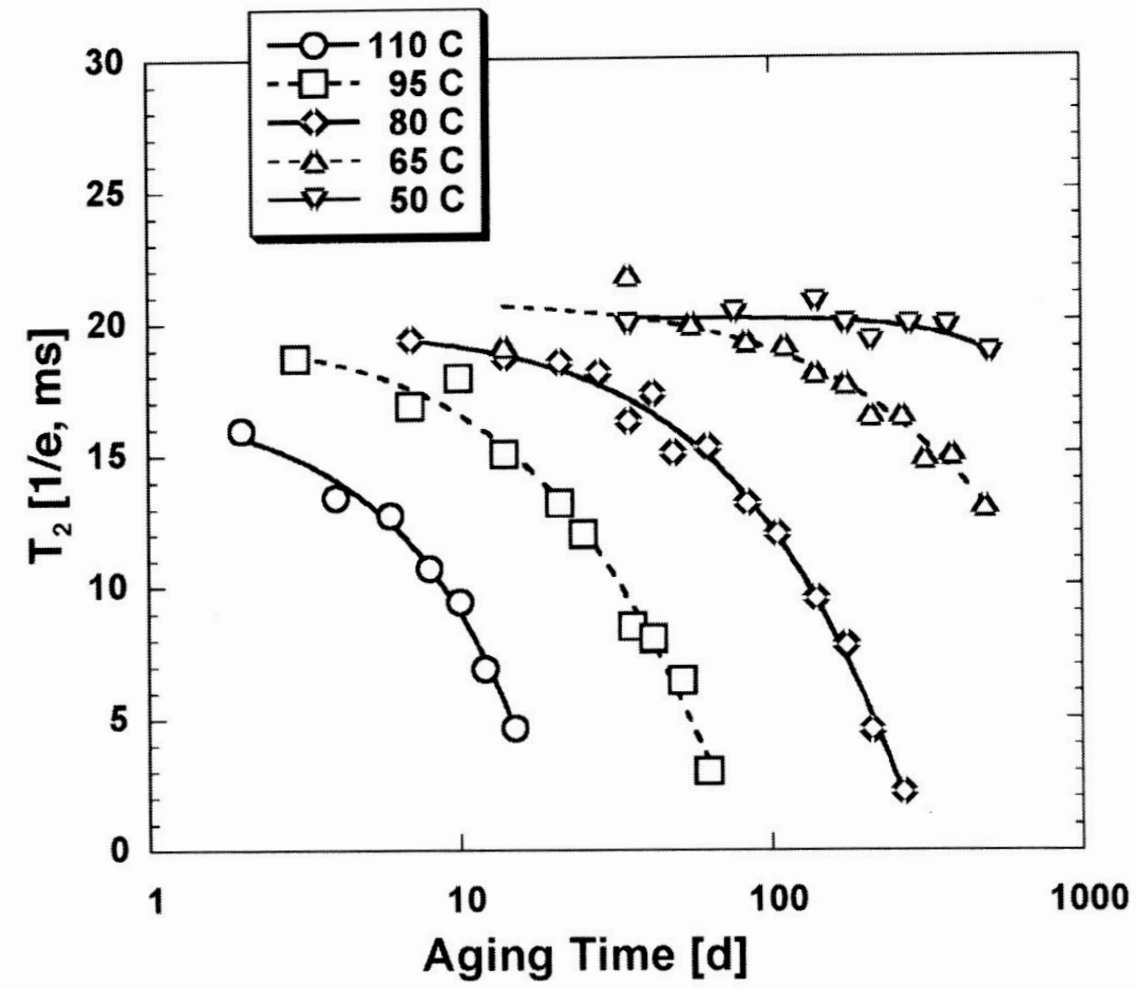

Figure 6. The ^{1}H NMR relaxation times of HTPB swollen in $CDCl_3$ as a function of aging time and temperature.

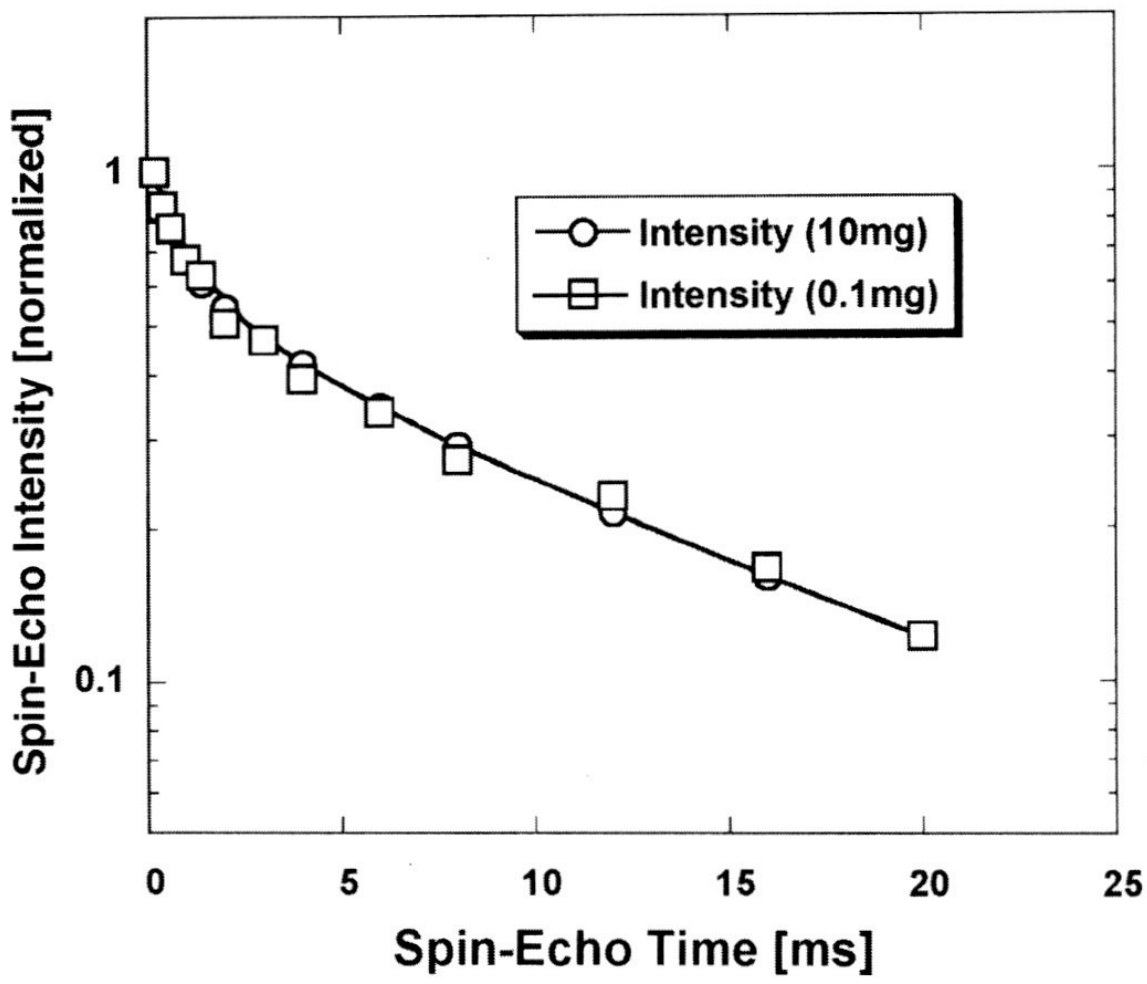

Figure 10. A comparison of the ^{1}H spin-echo decay curves of EPDM for 8 scans of a 10 mg sample and a single scan of a 0.1 mg sample.

Degradation Mechanisms (& Predictions)
Selective ^{13}C Labelling

Polyethylene

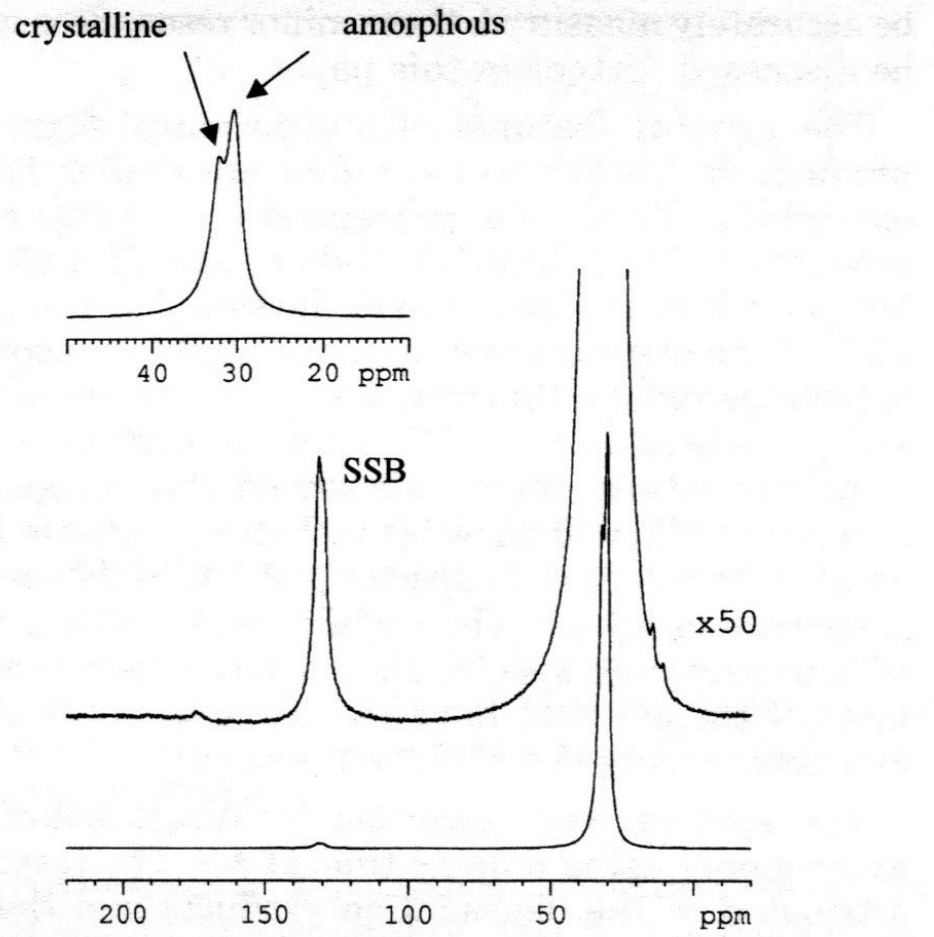

Figure 1. ^{13}C MAS NMR spectrum of unaged ^{13}C-polyethylene showing the crystalline and amorphous components of the main chain. SSB = spinning sideband.

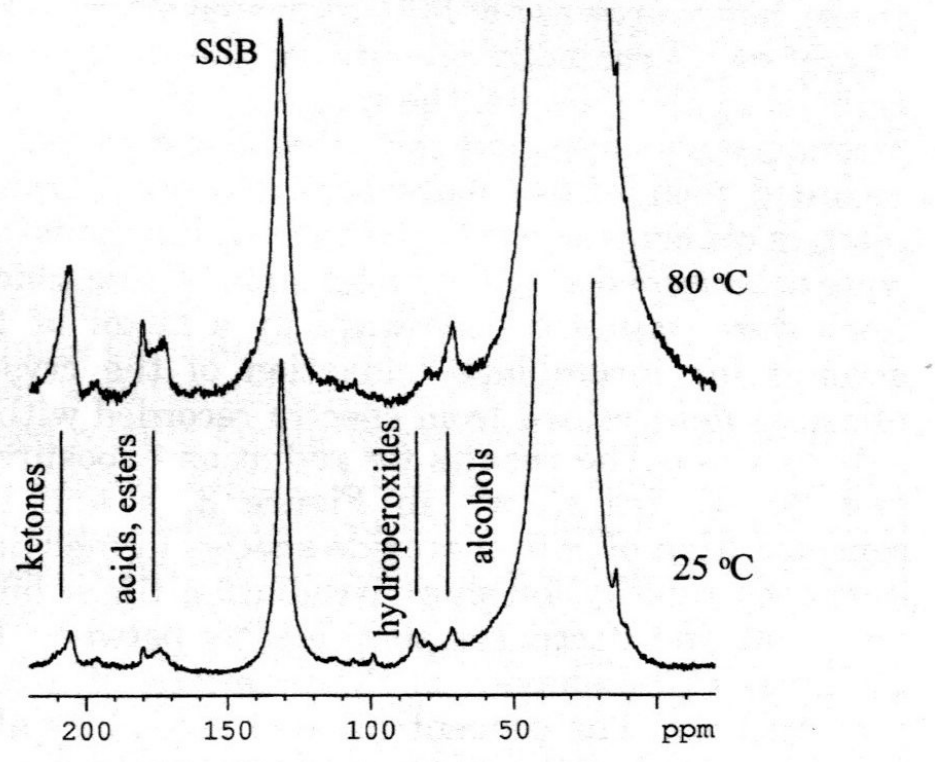

Figure 2. ^{13}C MAS NMR spectra of ^{13}C-polyethylene γ-irradiated for 7 days at 25 and 80 °C. Resonances corresponding to ketones, acids, esters, hydroperoxides, and alcohols are identified.

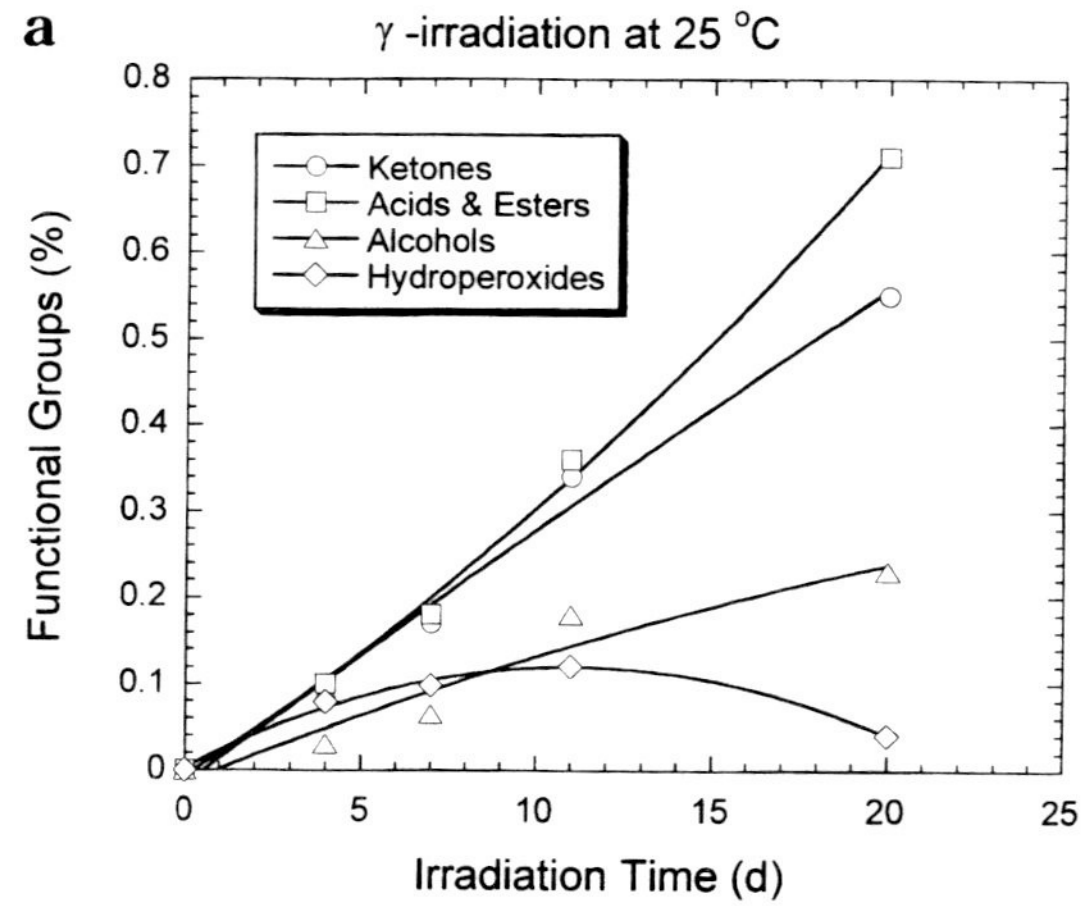

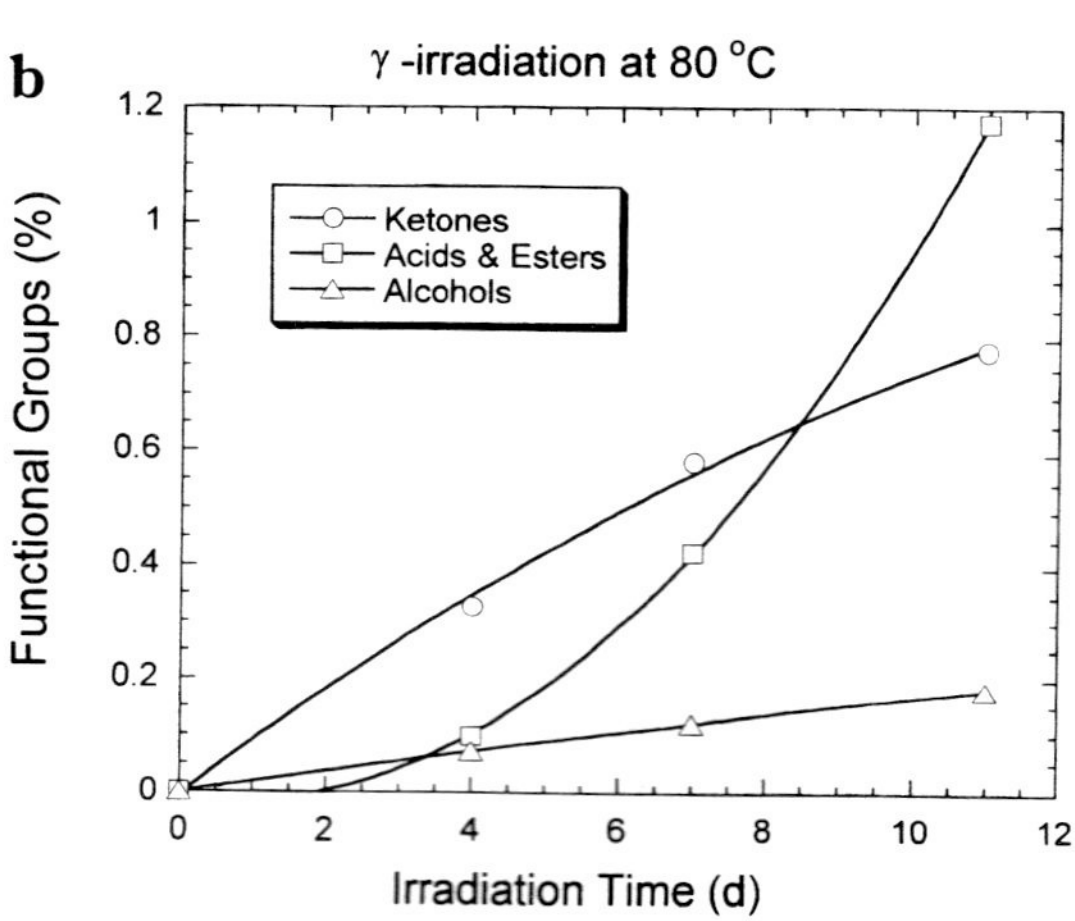

Figure 3. Distribution of functional groups vs irradiation time at (a) 25 and (b) 80 °C. The percents shown represent the percent carbons associated with each degradation species compared to the total carbon population.

Polypropylene

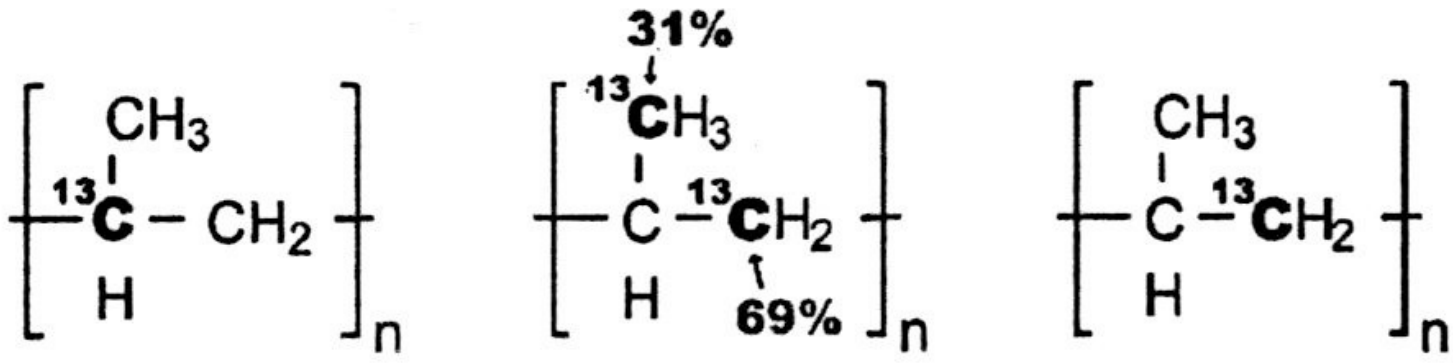

C(2) labeled

C(1,3) labeled

C(1) labeled

Scheme 1.

Table 1
Relative carbon-13 abundances[a] of chain carbons in selectively labeled PP materials

PP material	CH	CH_2	CH_3
C(1)	1.0 ± 0.2	96.7 ± 0.5	2.3 ± 0.3
C(1,3)	0.9 ± 0.1	68.3 ± 0.7	30.8 ± 0.6
C(2)	98.5 ± 0.3	0.8 ± 0.1	0.8 ± 0.1

[a]Determined with high-temperature, solution ^{13}C NMR spectroscopy. Samples of the PP powder were dissolved in 1,2,4-trichlorobenzene at 130 °C.

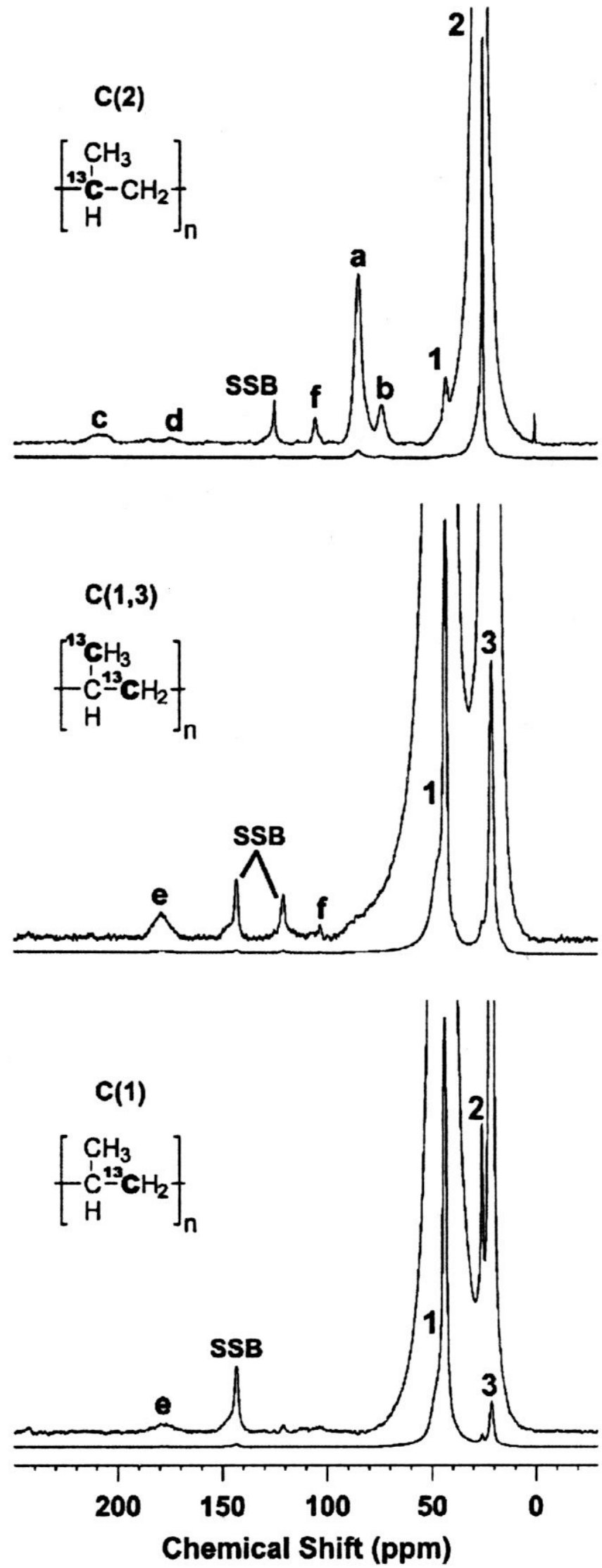
C(2)
CH3
13C
CH2
H
n
a
2
1
SSB
f
b
c
d
C(1,3)
13CH3
13C
13CH2
H
n
3
1
SSB
e
f
C(1)
CH3
13C
13CH2
H
n
2
1
SSB
e
3
200
150
100
50
0
Chemical Shift (ppm)

Table 2
^{13}C Resonances of oxidation-induced functional groups observed in solid-state NMR spectra of selectively labeled polypropylene samples

^{13}C chemical shift (ppm)	Oxidative functional group		PP position of origin	Aging conditions observed*
~215 (broad)	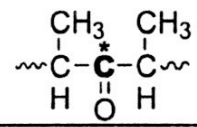	in-chain ketone	C(1)	γ (80 °C) γ' (109 °C)
~207 (broad)	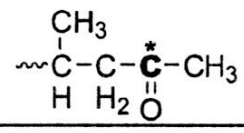	methyl (chain-end) ketone	C(2)	γ (24 °C, 80 °C) γ' (22 °C–109 °C)
~185 (broad)	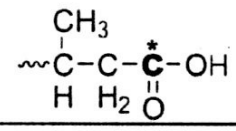	carboxylic acid	C(2)	γ (24 °C) γ' (22 °C)
~179 (broad)	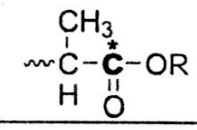	ester	C(1)	γ (24 °C, 80 °C) γ' (22 °C, 109 °C)
170–175 (broad)	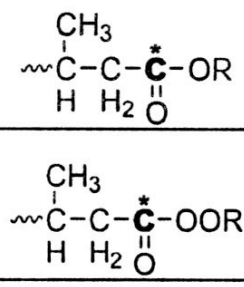	ester	C(2)	γ (24 °C, 80 °C) γ' (22 °C–109 °C)
		perester		
100–117 (several peaks)	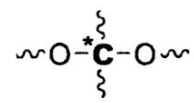	ketal	C(1) C(2)	γ (24 °C, 80 °C) γ' (22 °C–109 °C)
	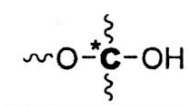	hemiketal		
85.3	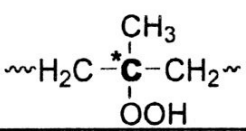	tertiary hydroperoxide	C(2)	γ (24 °C, 80 °C) γ' (22 °C–109 °C)
	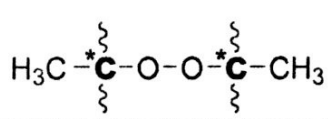	dialkyl peroxide		
74.2	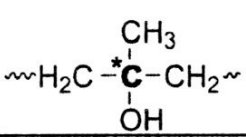	tertiary alcohol	C(2)	γ (24 °C, 80 °C) γ' (22 °C–109 °C)

*γ = exposure to γ-radiation in air; γ' = exposure to γ-radiation in 24 °C argon followed by post-irradiation thermal aging in air.

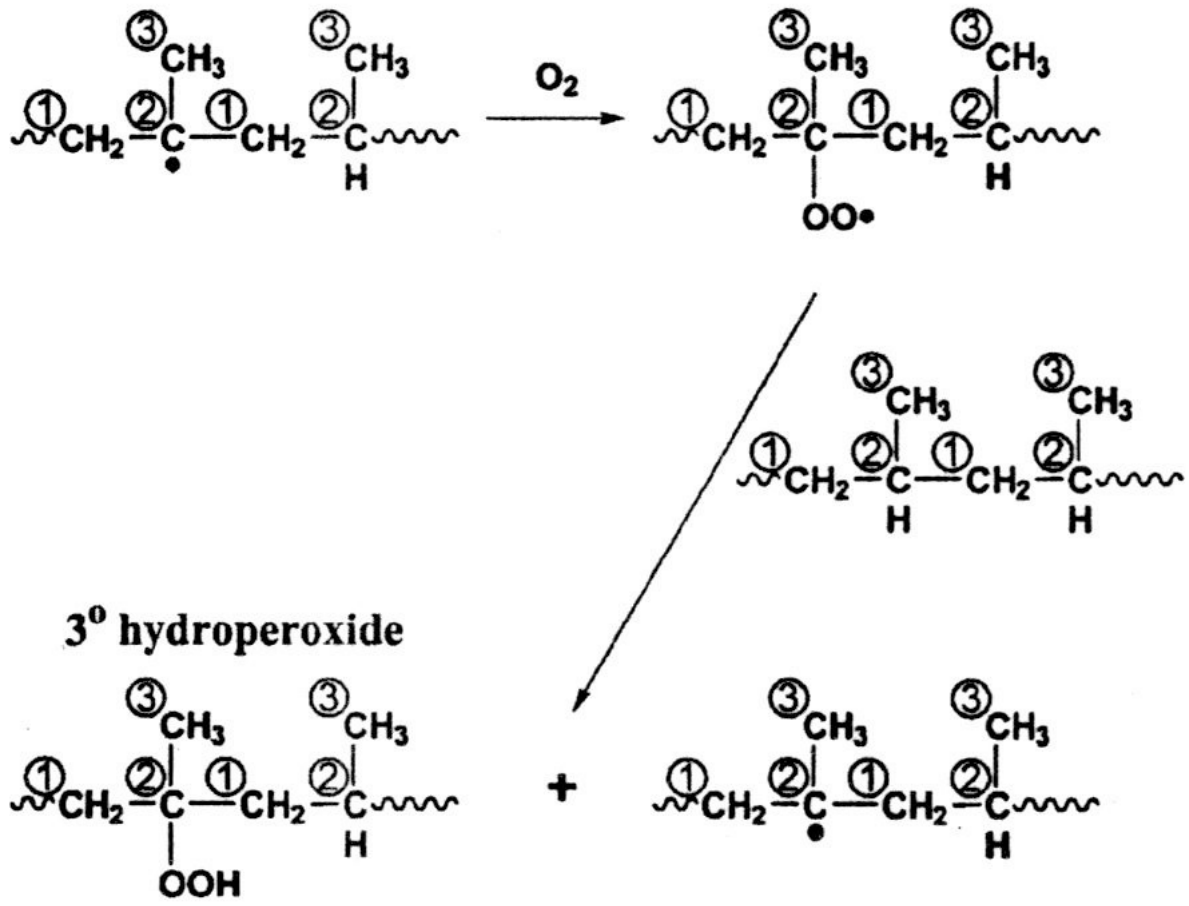

Scheme 2.

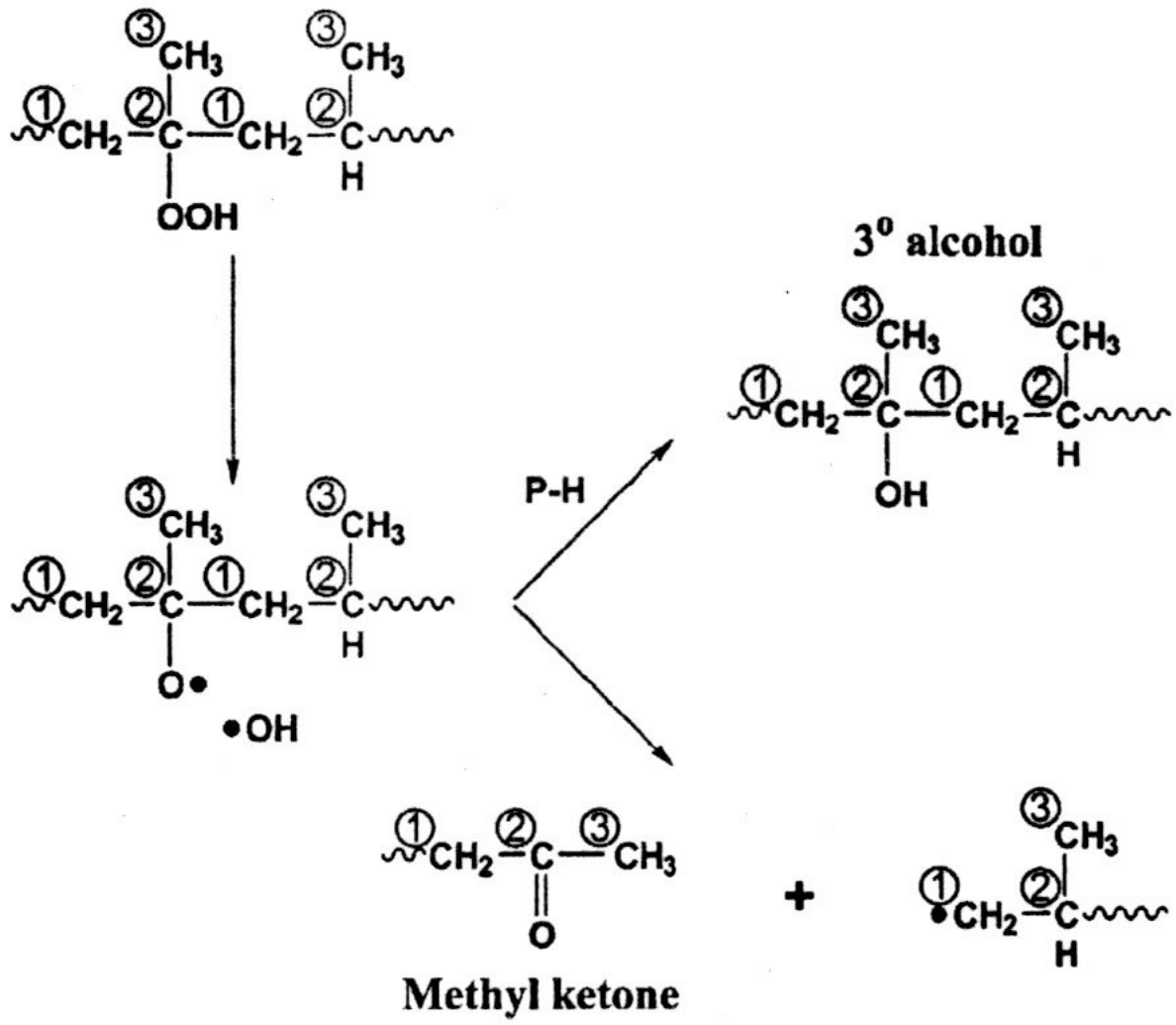

Radiation Sterilization - <u>Not</u>

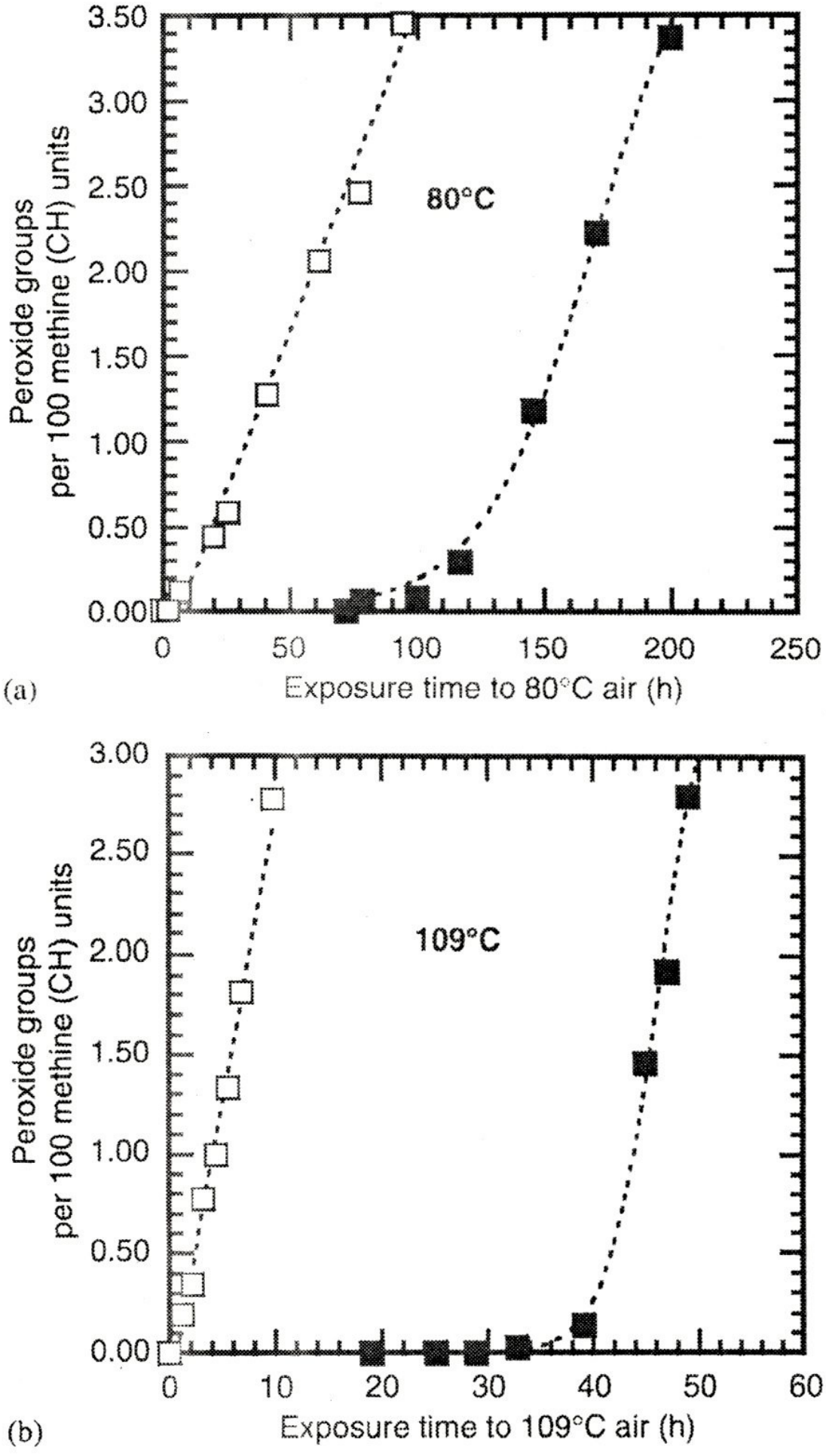

Fig. 9. Comparison of the kinetic accumulation of tertiary peroxide groups in solid C(2)-labeled polypropylene samples exposed to γ-radiation (240 kGy) in 24 °C argon followed by post-irradiation thermal aging in air (□) versus samples thermally aged in the absence of γ-radiation (■), at two different aging temperatures, (a) 80 °C and (b) 109 °C.

Oxygen Consumption

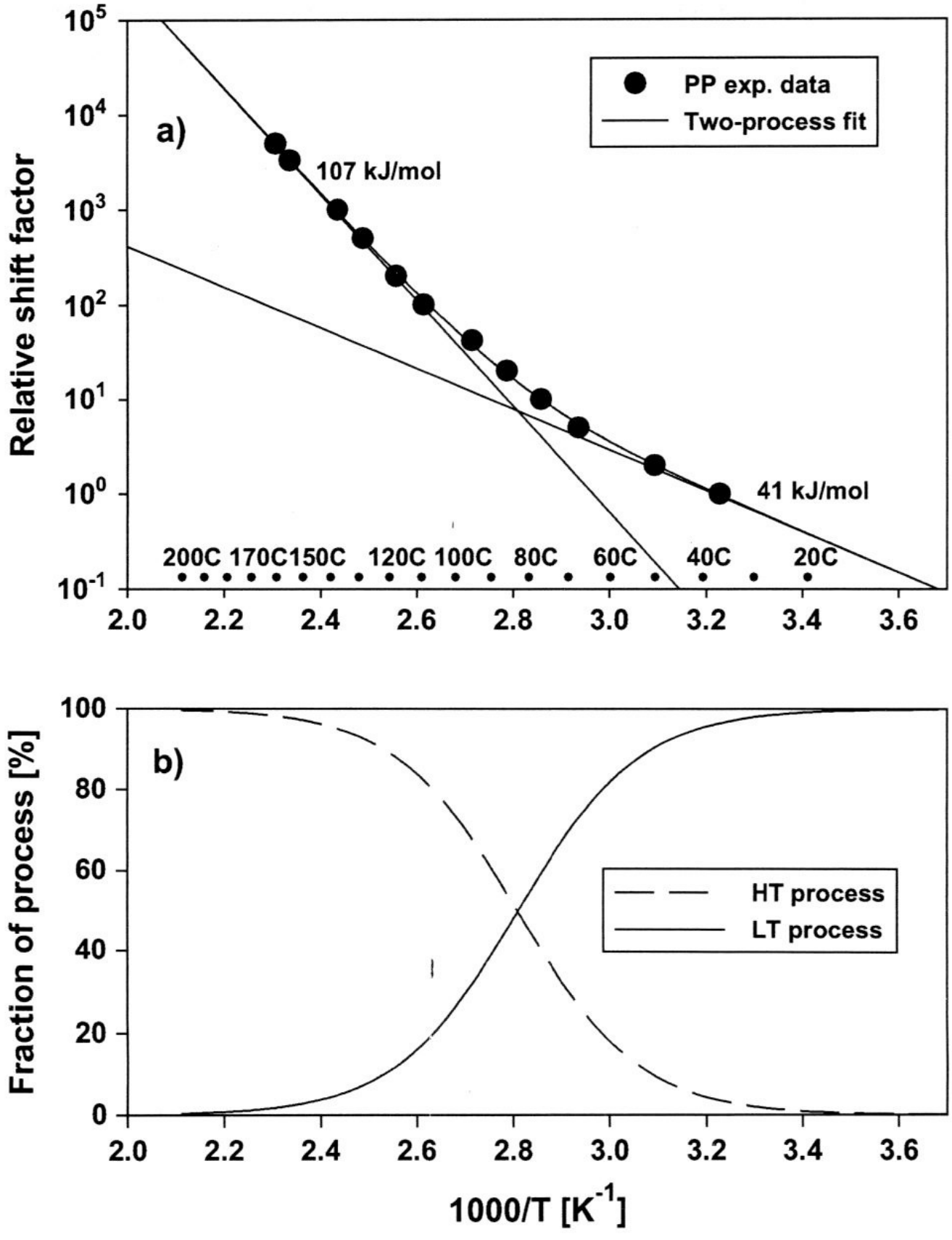

Fig. 5. (a) Curve fitting with two processes for PP [12], (b) relative contribution versus temperature.

Correlate Oxygen Consumption to Physical Properties

Suppose

- 1 month @ 160°C
  - 50% reduction in elongation
  - 1% gain in Oxygen content

- 1 months @ 25°C
  - 0.05% reduction in elongation
  - 0.001% gain in Oxygen content

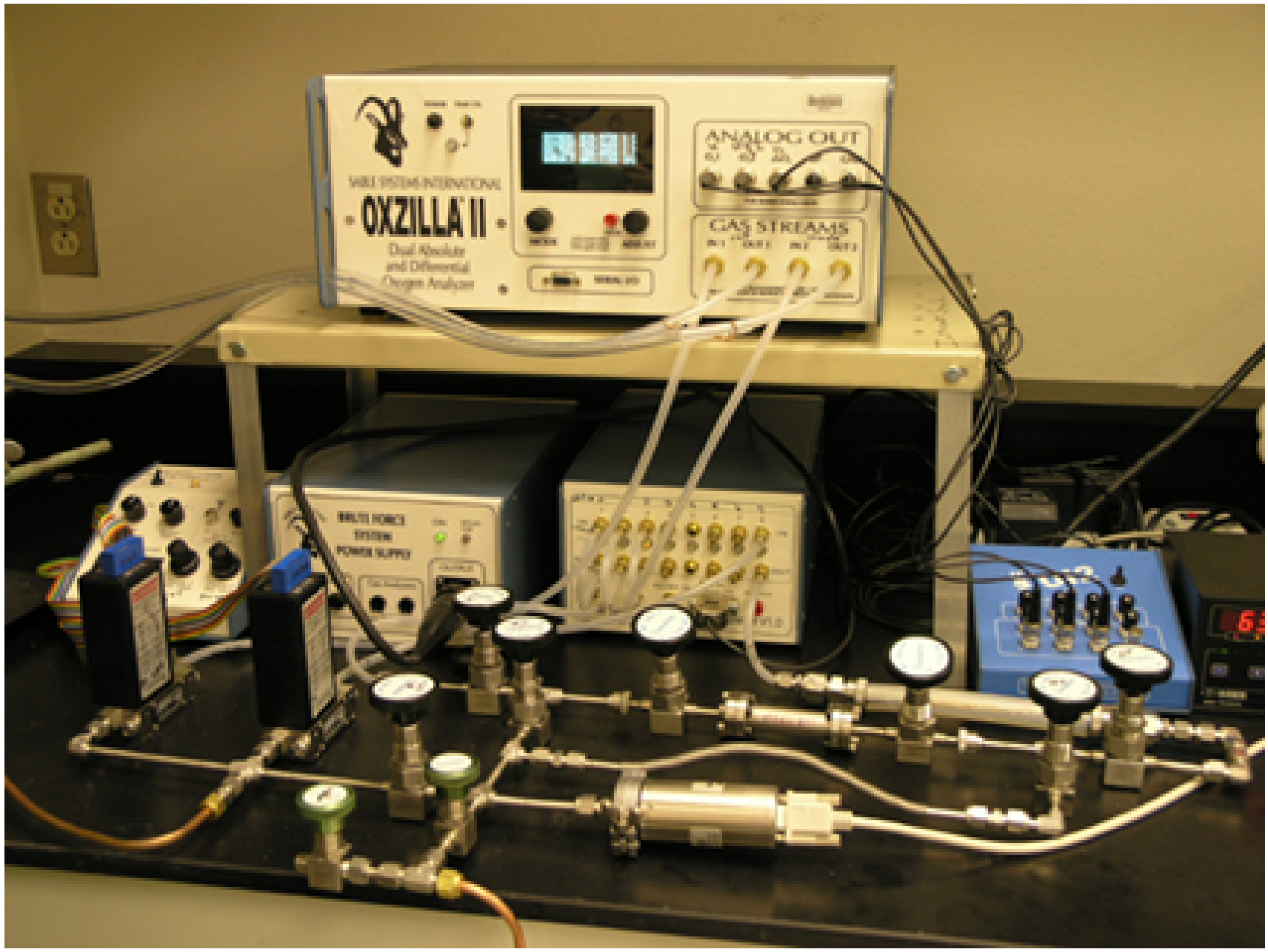
OXZILLA II
Dual Absolute
and Differential
Oxygen Analyzer
ANALOG OUT
GAS STREAMS

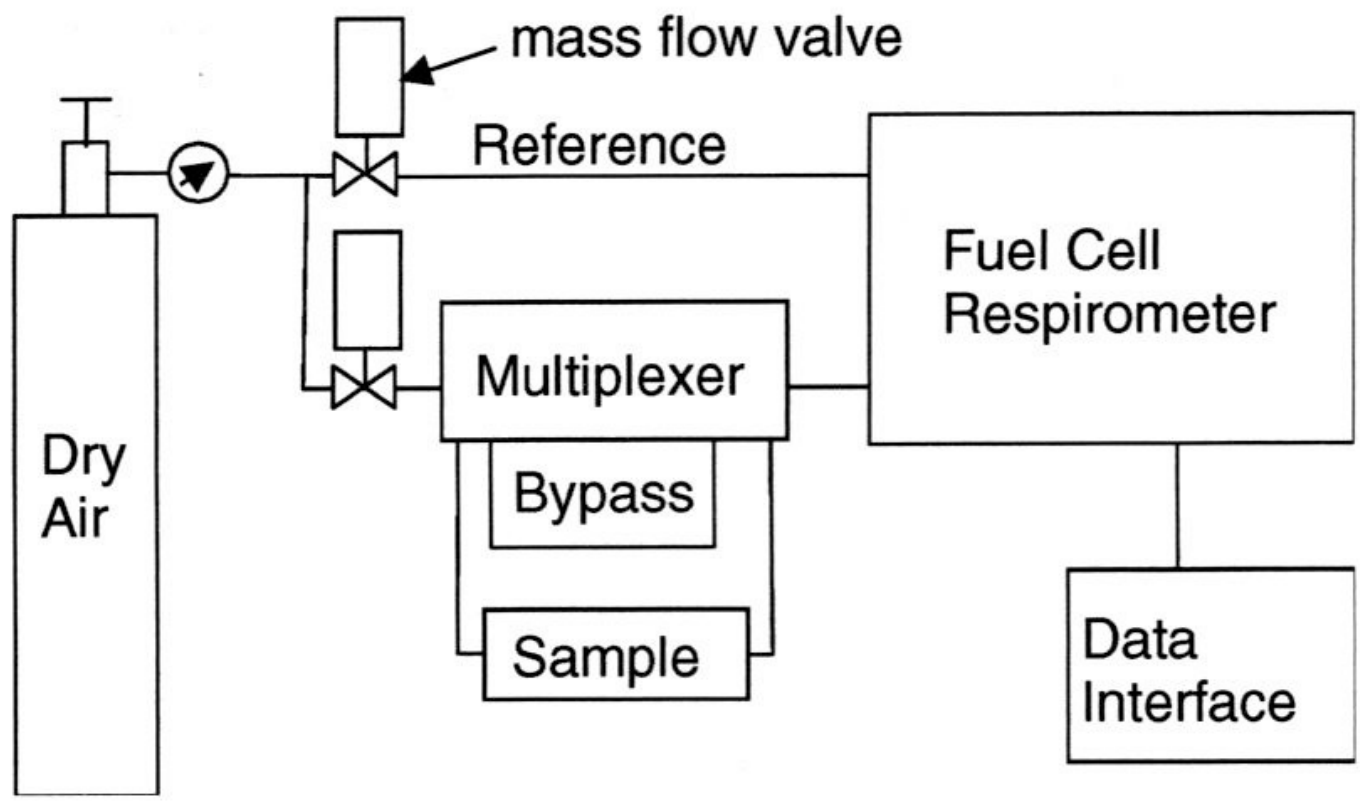
mass flow valve
Reference
Dry
Air
Multiplexer
Bypass
Sample
Fuel Cell
Respirometer
Data
Interface

Scheme 1.

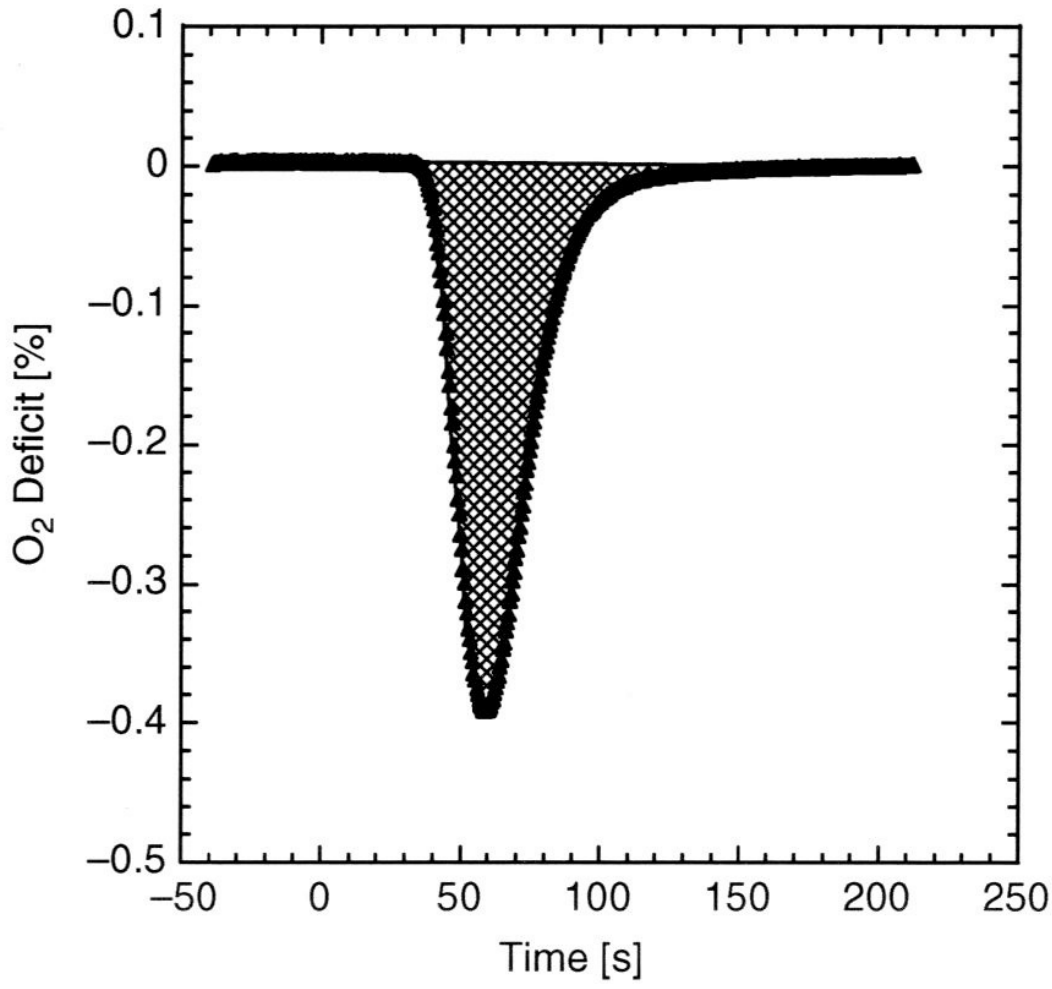

Fig. 1. The respirometer recording of the oxygen deficit trace of 0.207 g carbon filled natural rubber that has been aged for 16 h at 80 °C.

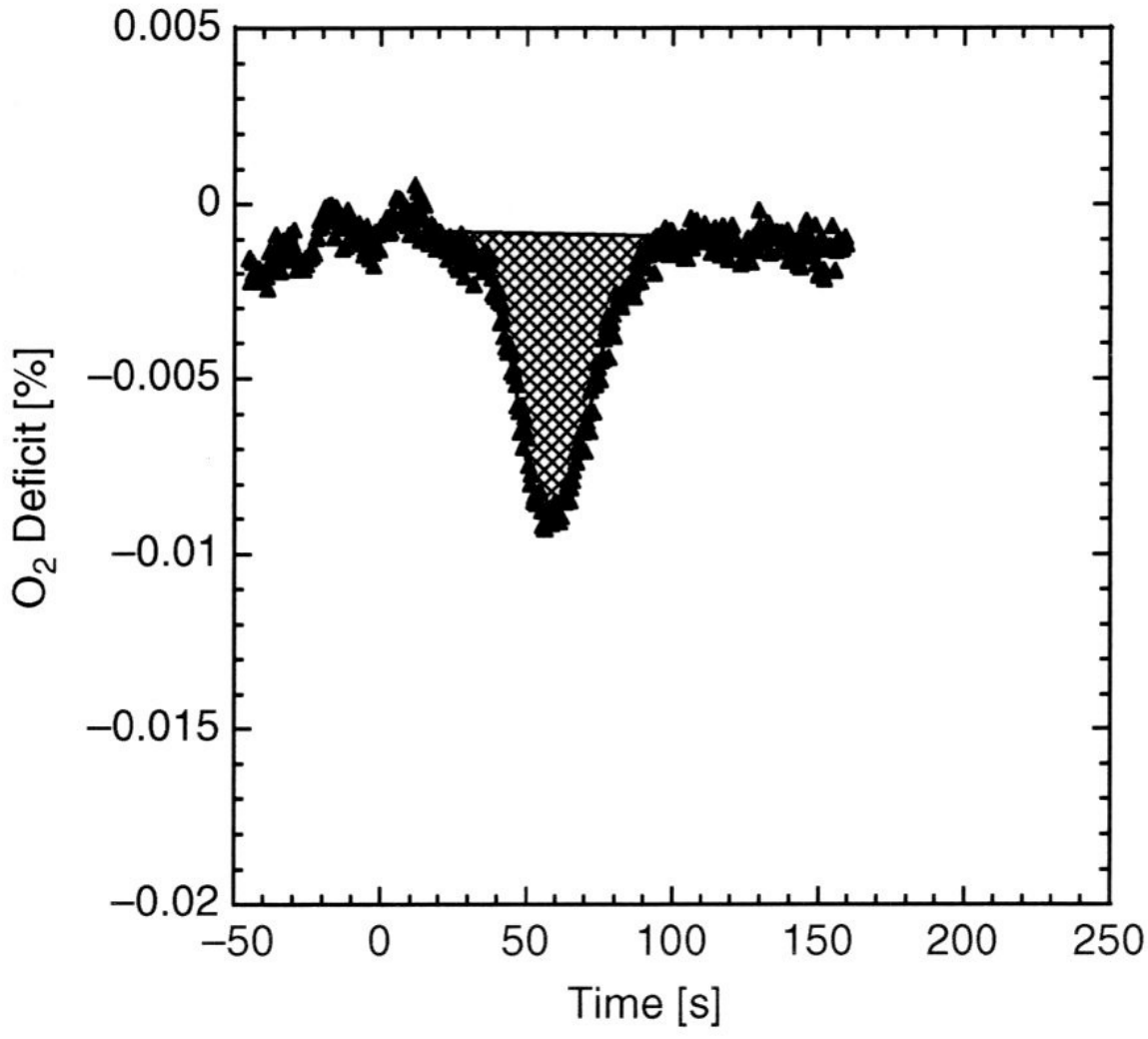

Fig. 2. The respirometer recording of the oxygen deficit trace of 1.07 g polyurethane foam that has been aged for 555 h at 23 °C.

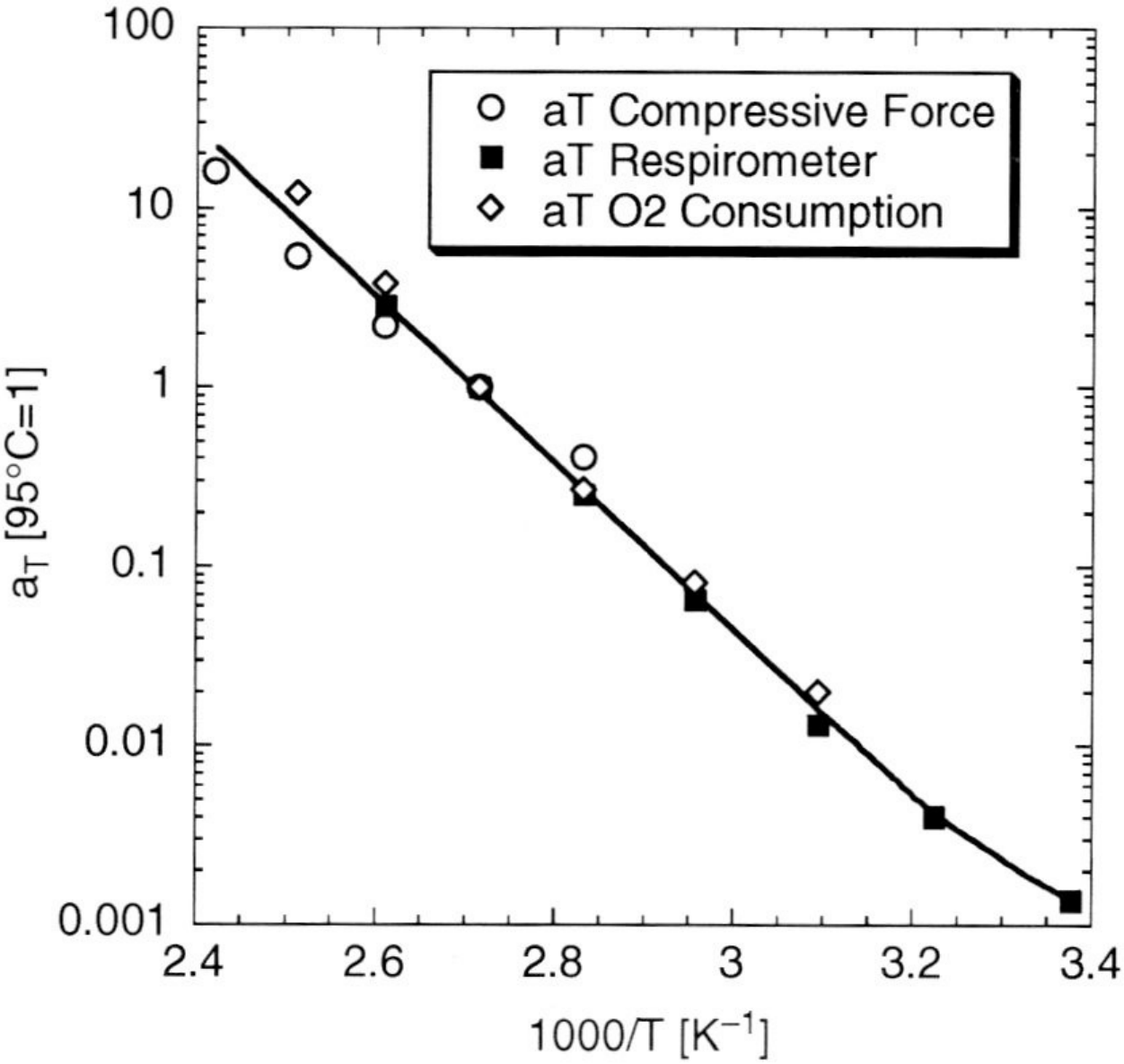

Fig. 10. The acceleration factors for the compressive force, the oxidation rate measured by the respirometer and the oxidation rate measured by UOC for a polyurethane foam.